CONCEPTUAL DESIGN OF RUBBLE MOUND BREAKWATERS

JENTSJE W. VAN DER MEER

This paper first gives an overall view of physical processes involved with rubble mound structures and a classification of these structures. Governing parameters are described as hydraulic parameters (related to waves, wave run-up and run-down, overtopping, transmission and reflection) and as structural parameters (related to waves, rock, cross-section and response of the structure). The description of hydraulic response is divided into:

- wave run-up and run-down,
- wave overtopping,
- wave transmission,
- wave reflection.

The main part of the paper describes the structural response (stability) which is divided into:

- rock armor layers,
- armor layers with concrete units,
- underlayers, filters, toe protection and head,
- low-crested structures,
- berm breakwaters.

The description of hydraulic and structural response is given in design formulas or graphs which can be used for a conceptual design of rubble mound structures.

1. Introduction

The design tools given in this paper on rubble mound structures are based on tests of schematized structures. Structures in prototype may differ (substantially) from the test-sections. Results based on these design tools can therefore only be used in a conceptual design. The confidence bands given for most formulas support the fact that reality may differ from the mean curve. It is advised to perform physical model investigations for detailed design of all important rubble mound structures.

1.1. *Processes involved with rubble mound structures*

The processes involved with stability of rubble mound structures under wave (possibly combined with current) attack are given in a basic scheme in Fig. 1.

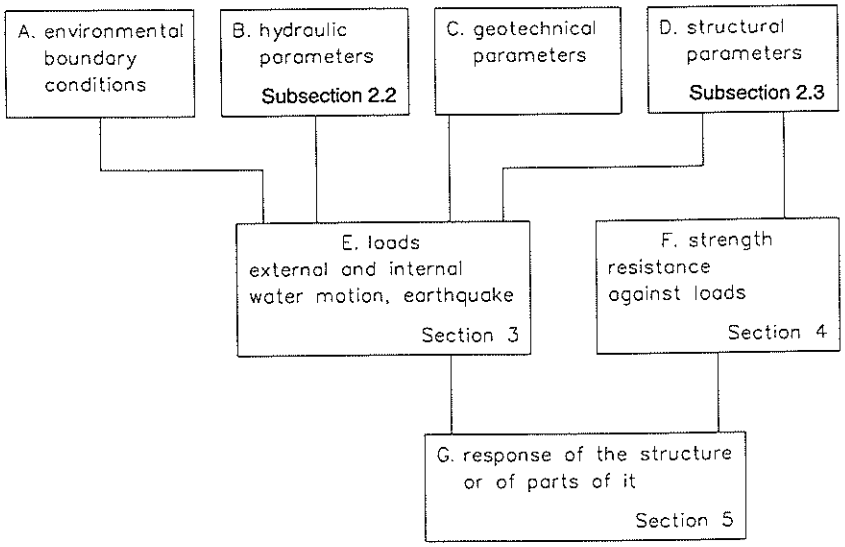

Fig. 1. Basic scheme of assessment of rubble mound structure response.

The environmental conditions (wave, current, and geotechnical characteristics) lead to a number of parameters which describe the boundary conditions at or in front of the structure (A in Fig. 1). These parameters are not affected by the structure itself, and generally, the designer of a structure has no influence on them. Wave height, wave height distribution, wave breaking, wave period, spectral shape, wave angle, currents, foreshore geometry, water depth, set-up and water levels are the main hydraulic environmental parameters. These environmental parameters are not described in this paper. A specific geotechnical environmental condition is an earthquake.

Governing parameters can be divided into parameters related to hydraulics (B in Fig. 1), related to geotechnics (C) and to the structure (D). Hydraulic parameters are related to the description of the wave action on the structure (hydraulic response). These hydraulic parameters are described in Subsecs. 2.1 and 2.2. The main hydraulic responses are wave run-up, run-down, wave overtopping, wave transmission and reflection. These are covered in Sec. 3.

Geotechnical parameters are related to, for instance, liquefaction, dynamic gradients, and excessive pore pressures. They are not described in this paper.

The structure can be described by a large number of structural parameters (D) and some important ones are the slope of the structure, the mass and mass density of the rock, rock or grain shape, surface smoothness, cohesion, porosity, permeability, shear and bulk moduli, and the dimensions and cross-section of the structure. The structural parameters related to hydraulic stability are described in Subsecs. 2.3.

The loads on the structure or on structural elements are given by the environmental, hydraulic, geotechnical, and structural parameters together (E in Fig. 1). These loads can be divided into those due to external water motion on the slope, loads generated by internal water motion in the structure, and earthquakes. The external water motion is affected amongst others things by the deformation of the wave (breaking or not breaking), the run-up and run-down, transmission, overtopping and reflection. These topics are described in Subsec. 2.2. The internal water motion describes the penetration or dissipation of water into the structure, the variation of pore pressures and the variation of the freatic line. These topics are not treated in this paper.

Almost all structural parameters might have some or large influence on the loads. Size, shape, and grading of armor stones have influence on the roughness of the slope, and therefore, on run-up and run-down. Filter size and grading, together with the above-mentioned characteristics of the armor stones, have an influence on the permeability of the structure, and hence, on the internal water motion.

The resistance against the loads (waves, earthquakes) can be called the strength of the structure (F in Fig. 1). Structural parameters are essential in the formulation of the strength of the structure. Most of them also influence the loads, as described above.

Finally the comparison of the strength with the loads leads to a description of the response of the structure or elements of the structure (G in Fig. 1), the description of the so-called failure mechanisms. The failure mechanism may be treated in a deterministic or probabilistic way.

Hydraulic structural responses are stability of armor layers, filter layers, crest and rear, toe berms, and stability of crest walls and dynamically stable slopes. These structural responses are described in Sec. 4. Geotechnical responses or interactions are slip failure, settlement, liquefaction, dynamic response, internal erosion, and impacts. They are not described in this paper.

Figure 1 can also be used in order to describe the various ways of physical and numerical modeling of the stability of coastal and shoreline structures. A black box method is used if the environmental parameters (A in Fig. 1) and the hydraulic (B) and structural (D) parameters are modeled physically, and the responses (G) are given in graphs or formulas. A description of water motion (E) and strength (F) is not considered.

A grey box method is used if parts of the loads (E) are described by theoretical formulations or numerical models which are related to the strength (F) of the structure by means of a failure criterion or reliability function. The theoretical derivation of a stability formula might be the simplest example of this.

Finally, a white box is used if all relevant loads and failure criterions can be described by theoretical/physical formulations or numerical models, without empirical constants. It is obvious that it will take a long time and a lengthy research effort before coastal and shoreline structures can be designed by means of a white box.

The colors black, grey, and white, used for the methods described above do not suggest a preference. Each method can be useful in a design procedure.

This paper will deal with physical processes and design tools, which means that design tools should be described so that

- they are easily applicable;
- the range of application should be as wide as possible;
- research data from various investigations should, wherever possible, be combined and compared, rather than giving the data of different investigations separately.

1.2. *Classification of rubble mound structures*

Rubble mound structures can be classified by the use of the $H/\Delta D$ parameter, where H = wave height, Δ = relative mass density, and D = characteristic diameter of structure, armor unit (rock or concrete), stone, shingle, or sand. Small values of $H/\Delta D$ give structures as caissons or structures with large armor units. Large ones imply gravel beaches and sand beaches.

Only two types of structures have to be distinguished if the response of the various structures is concerned. These types can be classified into statically stable and dynamically stable.

Statically stable structures are those where no or minor damage is allowed under design conditions. Damage is defined as displacement of armor units. The mass of individual units must be large enough to withstand the wave forces during design conditions. Caissons and traditionally designed breakwaters belong to the group of statically stable structures. The design is based on an optimum solution between design conditions, allowable damage, and cost of construction and maintenance. Static stability is characterised by the design parameter damage, and can roughly be classified by $H/\Delta D = 1$–4.

Dynamically stable structures are structures where profile development is concerned. Units (stones, gravel, or sand) are displaced by wave action until a profile is reached where the transport capacity along the profile is reduced to a very low level. Material around the still-water level is continuously moving during each run-up and run-down of the waves, but when the net transport capacity has become zero, the profile has reached an equilibrium. Dynamic stability is characterised by the design parameter profile, and can roughly be classified by $H/\Delta D > 6$.

The structures concerned in this paper are rock armored breakwaters and slopes and berm type breakwaters. The structures are roughly classified by $H/\Delta D$ =1–10.

An overview of the types of structures with different $H/\Delta D$ values is shown in Fig. 2, which gives the following rough classification:

1. $H/\Delta D < 1$ Caissons or seawalls.
   No damage is allowed for these fixed structures. The diameter, D, can be the height or width of the structure.
2. $H/\Delta D = 1$–4 Stable breakwaters.
   Generally uniform slopes are applied with heavy artificial armor units or natural rock. Only little damage (displacement) is allowed under severe design conditions. The diameter is a characteristic diameter of the unit, such as the nominal diameter.
3. $H/\Delta D = 3$–6 S-shaped and berm breakwaters.
   These structures are characterised by more or less steep slopes above and below the still-water level with a more gentle slope in between which reduces the wave forces on the armor units. Berm breakwaters are designed with a very steep seaward slope and a horizontal berm just above the still-water level. The first storms develop a more gentle profile which is stable further on. The profile changes to be expected are important.
4. $H/\Delta D = 6$–20 Rock slopes/beaches.
   The diameter of the rock is relatively small and cannot withstand severe wave attack without displacement of material. The profile which is being developed under different wave boundary conditions is the design parameter.

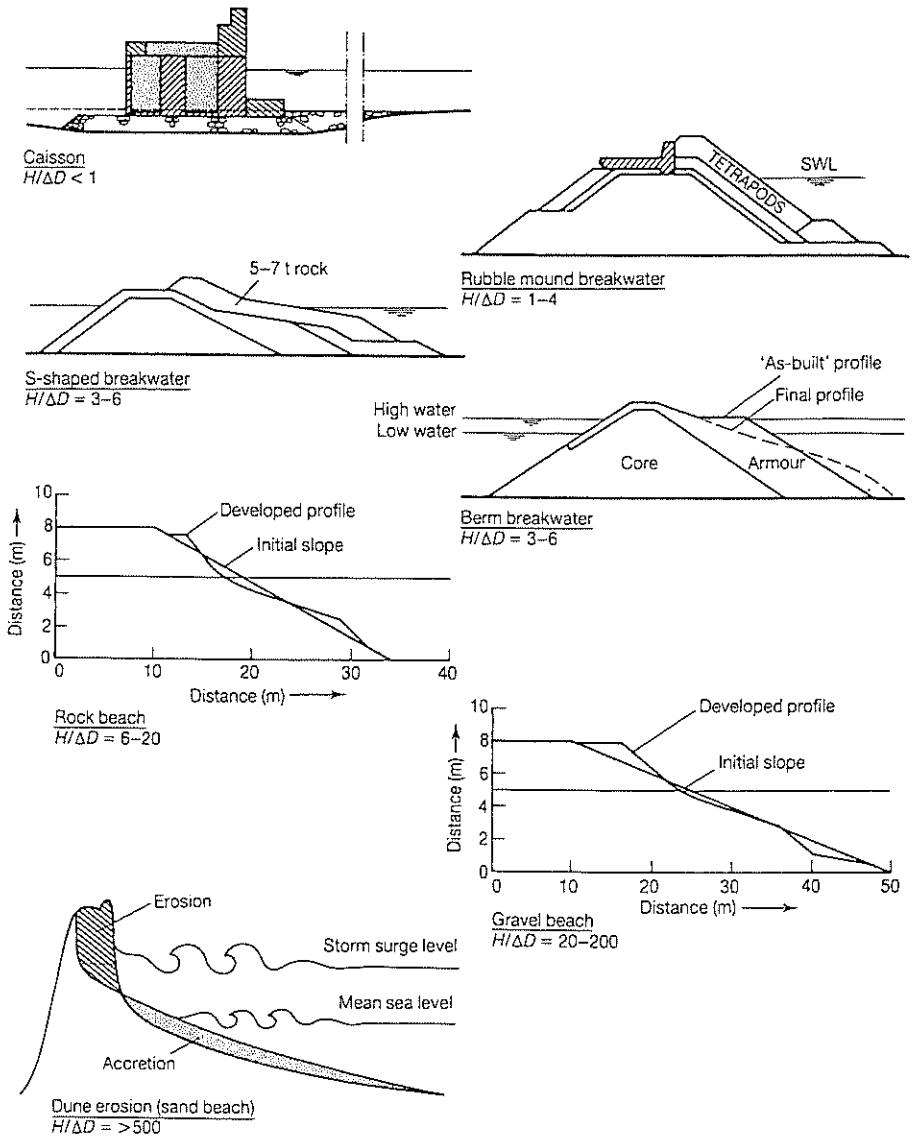

Fig. 2. Type of structure as a function of $H/\Delta D$.

5. $H/\Delta D = 15$–500 Gravel beaches.
   Grain sizes, roughly between ten centimeters and four millimeters, can be classified as gravel. Gravel beaches will change continuously under varying wave conditions and water levels (tide). Again the development of the profile is one of the design parameters.
6. $H/\Delta D > 500$ Sand beaches (during storm surges).
   Also material with very small diameters can withstand severe wave attack. The Dutch coast is partly protected by sand dunes. The dune erosion and profile development during storm surges is one of the main design parameters. Extensive basic research has been performed on this topic (Vellinga, 1986 and Steetzel, 1993).

2. Governing Parameters

The wave boundary conditions can mainly be described by the wave height, period, or steepness and the surf similarity parameter.

The main hydraulic responses of rubble mound structures to wave conditions are wave run-up and run-down, overtopping, transmission, and reflection. The governing parameters related to these hydraulic responses are illustrated in Fig. 3, and are discussed in this section. The hydraulic responses itself are described in Sec. 3.

Finally, a large number of structural parameters can be defined, related to waves, rock, the cross-section and the response of the structure. The structural parameters are treated in this section, the structural responses in Sec. 4.

2.1. *Wave parameters*

Wave conditions are given principally by the incident wave height at the toe of the structure, H, usually as the significant wave height, H_s (average of the highest 1/3 of the waves) or $H_{m0}(4\sqrt{m_0}$, based on the spectrum); the mean or peak wave periods, T_m or T_p (based on statistical or spectral analysis); the angle of wave attack, β, and the water depth, h.

The wave height distribution at deep water can be described by the Rayleigh distribution and in that case one characteristic value, for instance, the significant wave height, describes the whole distribution. In shallow and depth limited water, the highest waves break and in most cases the wave height distributions can no longer be described by the Rayleigh distribution. In those situations, the actual wave height distribution may be important to consider,

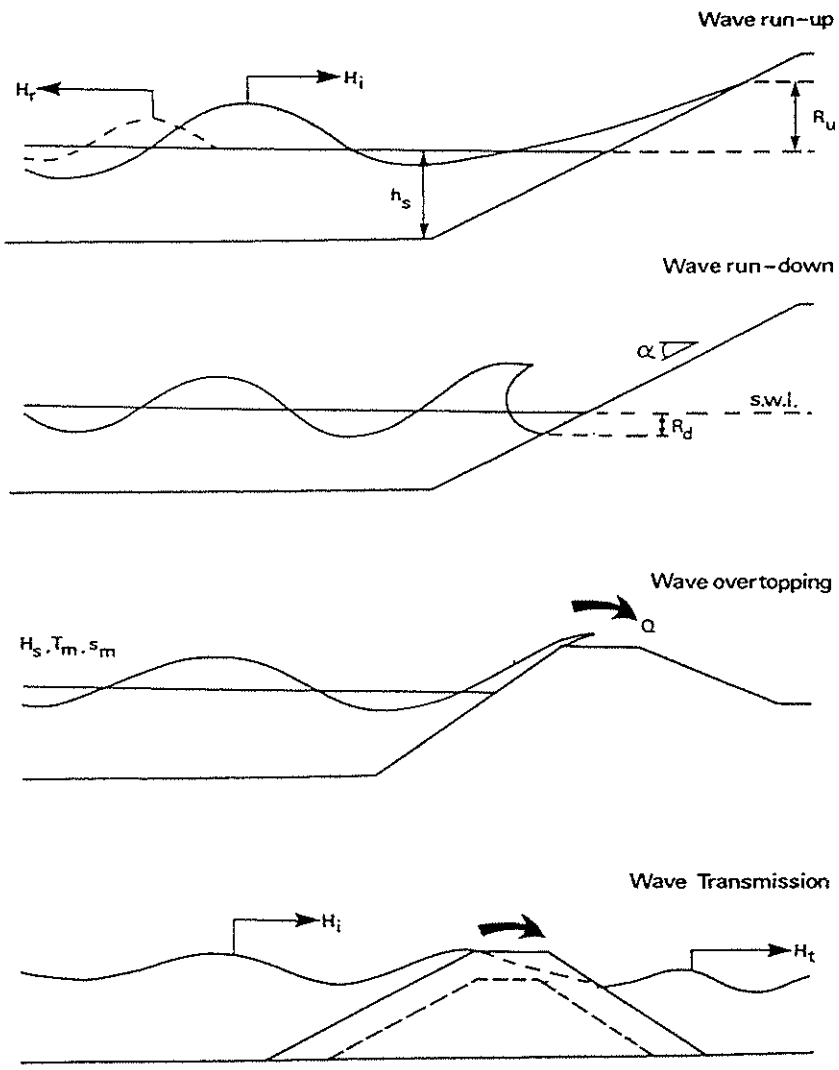

Fig. 3. Governing hydraulic parameters.

or another characteristic value other than the significant wave height. Characteristic values often used are the 2% wave height, $H_{2\%}$, and the $H_{1/10}$, being the average of the highest ten percent of the waves. For a Rayleigh distribution, the values $H_{2\%} = 1.4\ H_s$ and $H_{1/10} = 1.27\ H_s$ hold.

The influence of the wave period is often described as a wave length and related to the wave height, resulting in a wave steepness. The wave steepness, s, can be defined by using the deep water wave length, $L = gT^2/2\pi$:

$$s = \frac{2\pi H}{gT^2} \tag{1}$$

If the situation considered is not really in deep water (in most cases), the wave length at deep water and at the structure differ and therefore, a fictitious wave steepness is obtained. In fact, the wave steepness as defined in Eq. (1) describes a dimensionless wave period. Use of H_s and T_m or T_p in Eq. 1 gives a subscript to s, respectively s_{om} and s_{op}.

The most useful parameter describing wave action on a slope, and some of its effects, is the surf similarity or breaker parameter, ξ, also termed the Iribarren number Ir:

$$\xi = \tan\alpha/\sqrt{s} \tag{2}$$

The surf similarity parameter has often been used to describe the form of wave breaking on a beach or structure (see Fig. 4). It should be noted that

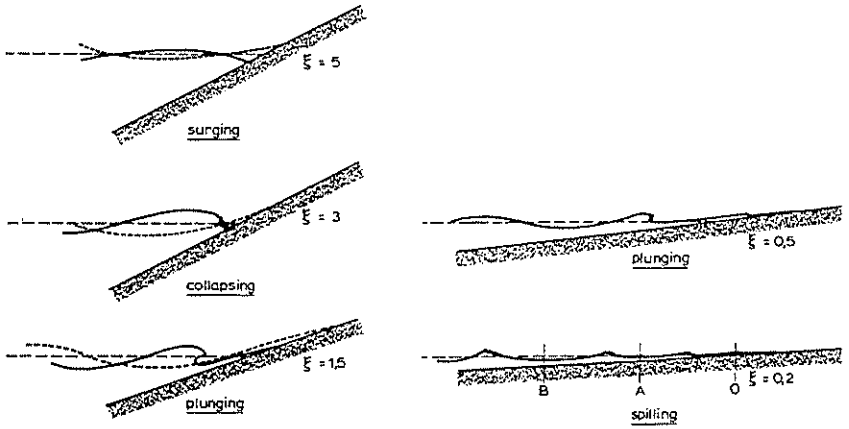

Fig. 4. Breaker types as a function of ξ. (Battjes, 1974)

different versions of this parameter are defined within this paper, reflecting the approaches of different researchers. In this section, ξ_m and ξ_p are used when s is described by s_{om} or s_{op}.

2.2. *Hydraulic parameters*

2.2.1. *Run-up and run-down*

Wave action on a rubble mound structure will cause the water surface to oscillate over a vertical range generally greater than the incident wave height. The extreme levels reached in each wave, termed run-up and run-down, R_u and R_d respectively, and defined relative to the static water level, constitute important design parameters (see Fig. 3). The design run-up level will be used to determine the level of the structure crest, the upper limit of protection or other structural elements, or as an indicator of possible overtopping or wave transmission. The run-down level is often taken to determine the lower extent of main armor protection and/or a possible level for a toe berm.

Run-up and run-down are often given in a dimensionless form, R_{ux}/H_s and R_{dx}/H_s, where the subscript x describes the level considered (for instance 2%) or significant (s).

2.2.2. *Overtopping*

If extreme run-up levels exceed the crest level, the structure will overtop. This may occur for relatively few waves under the design event, and a low overtopping rate may often be accepted without severe consequences for the structure or the area protected by it. Sea walls and breakwaters are often designed on the basis that some (small) overtopping discharge is to be expected under extreme wave conditions. The main design problem therefore reduces to one of dimensioning the cross-section geometry such that the mean overtopping discharge, q, under design conditions remains below acceptable limits.

The most simple dimensionless parameter, Q, for the mean overtopping discharge, q, can be defined by

$$Q = \frac{q}{\sqrt{gH_s^3}} \tag{3}$$

Sometimes the wave steepness and slope angle also have influence on the overtopping and in that case, the definition of dimensionless overtopping discharge as in Eq. (3) may be extended by including s_{om} or s_{op} and/or $\cot\alpha$. Various definitions can be found in Owen (1980), Bradbury *et al.* (1988), and De Waal and Van der Meer (1992).

2.2.3. *Wave transmission*

Breakwaters with relatively low crest levels may be overtopped with sufficient severity to excite wave action behind. Where a breakwater is constructed of relatively permeable construction, long wave periods may lead to transmission of wave energy through the structure. In some cases, the two different responses will be combined.

The quantification of wave transmission is important in the design of low-crested breakwaters intended to protect beaches or shorelines, and in the design of harbor breakwaters where long wave periods transmitted through the breakwater could cause movement of ships or other floating bodies.

The severity of wave transmission is described by the coefficient of transmission, C_t, defined in terms of the incident and transmitted wave heights, H_i and H_t respectively, or the total incident and transmitted wave energies, E_i and E_t:

$$C_t = \frac{H_t}{H_i} = \sqrt{\frac{E_t}{E_i}} \tag{4}$$

2.2.4. *Wave reflections*

Wave reflections are of importance on the open coast, and at commercial and small boat harbours. The interaction of incident and reflected waves often lead to a confused sea in front of the structure, with occasional steep and unstable waves of considerable hazard to small boats. Reflected waves can also propagate into areas of a harbor previously sheltered from wave action. They will lead to increased peak orbital velocities, increasing the likelihood of movement of beach material. Under oblique waves, reflection will increase littoral currents and hence local sediment transport.

All coastal structures reflect some proportion of the incident wave energy. This is often described by a reflection coefficient, C_r, defined in terms of the incident and reflected wave heights, H_i and H_r respectively, or the total incident and reflected wave energies, E_i and E_r:

$$C_r = \frac{H_r}{H_i} = \sqrt{\frac{E_r}{E_i}} \tag{5}$$

When considering random waves, values of C_r may be defined using the significant incident and reflected wave heights as representative of the incident and reflected energies.

2.3. *Structural parameters*

Structural parameters can be divided into four categories which will be treated in this section, and are related to:

- waves;
- rock;
- the cross-section; and
- the response of the structure.

2.3.1. *Structural parameters related to waves*

The most important parameter which gives a relationship between the structure and the wave conditions has been used in Subsec. 1.2. In general, the $H/\Delta D$ gives a good classification. For the design of rubble mound structures, this parameter should be defined in more detail.

The wave height is usually the significant wave height, H_s, defined either by the average of the highest one third of the waves or by $4\sqrt{m_0}$. For deep water, both definitions give more or less the same wave height. For shallow water conditions substantial differences may be present.

The relative buoyant density is described by

$$\Delta = \frac{\rho_r}{\rho_w} - 1 \tag{6}$$

where,

ρ_r = mass density of the rock (saturated surface dry mass density),

ρ_w = mass density of water.

The diameter used is related to the average mass of the rock and is called the nominal diameter:

$$D_{n50} = \left(\frac{M_{50}}{\rho_r}\right)^{1/3} \tag{7}$$

where,

D_{n50} = nominal diameter,

M_{50} = median mass of unit given by 50% on mass distribution curve.

The parameter $H/\Delta D$ changes to $H_s/\Delta D_{n50}$.

Another important structural parameter is the surf similarity paramete which relates the slope angle to the wave period or wave steepness, and whi gives a classification of breaker types. The surf similarity parameter $\xi(\xi_m, \xi$ with T_m, T_p) is defined in Subsec. 2.1.

For dynamically stable structures with profile development, a surf similari parameter cannot be defined as the slope is not straight. Furthermore, dynan ically stable structures are described by a large range of $H_s/\Delta D_{n50}$ values. I that case, it is possible to also relate the wave period to the nominal diamet and to make a combined wave height – period parameter. This parameter defined by

$$H_o T_o = \frac{H_s}{\Delta D_{n50}} * T_m \sqrt{\frac{g}{D_{n50}}} \tag{(}$$

The relationship between $H_s/\Delta D_{n50}$ and $H_o T_o$ is listed in Table 1.

Table 1. Relationship between $H_s/\Delta D_{n50}$ and $H_o T_o$.

Structure	$H_s/\Delta D_{n50}$	$H_o T_o$
Statically stable breakwaters	1–4	< 100
Rock slopes and beaches	6–20	200–1500
Gravel beaches	15–500	1000–200,000
Sand beaches	> 500	$> 200,000$

Another parameter which relates both wave height and period (or wa steepness) to the nominal diameter was introduced by Ahrens (1987). In tl Shore Protection Manual (SPM, 1984), $H_s/\Delta D_{n50}$ is often called the stabili number, N_s. Ahrens included the local wave steepness in a modified stabili number, N_s^*, defined by

$$N_s^* = N_s s_p^{-1/3} = \frac{H_s}{\Delta D_{n50}} s_p^{-1/3} \tag{(}$$

In this equation, s_p is the local wave steepness and not the deep water wave steepness. The local wave steepness is calculated using the local wave length from the Airy theory, where the deep water wave steepness is calculated by Eq. (1). This modified stability number, N_s^*, has a close relationship with $H_o T_o$

Table 2. Wave height-period parameters.

$$\frac{H_s}{\Delta D_{n50}} = N_s$$

$$\frac{H_s}{\Delta D_{n50}} s_p^{-1/3} = N_s^*$$

$$\frac{H_s}{\Delta D_{n50}} T_m \sqrt{\frac{g}{D_{n50}}} = H_o T_o$$

$$\frac{H_s}{\Delta D_{n50}} s_m^{-0.5} \sqrt{\frac{2\pi H_s}{D_{n50}}} = H_o T_o$$

$$\xi_m = \frac{\tan\alpha}{\sqrt{s_{om}}} = \frac{\tan\alpha}{\sqrt{\frac{2\pi H_s}{g T_m^2}}}$$

defined by Eq. (8). An overview of possible wave height-period parameters is given in Table 2.

2.3.2. *Structural parameters related to rock*

The most important parameter which is related to the rock is the nominal diameter defined by Eq. (7). Related to this is, of course, M_{50}, the 50% value on the mass distribution curve. The grading of the rock can be given by the D_{85}/D_{15}, where D_{85} and D_{15} are the 85% and 15% values of the sieve curves, respectively, or by D_{n85}/D_{n15}, based again on the mass distribution curves. These are the most important parameters as far as stability of armor layers is concerned. Examples of gradings are shown in Table 3, showing the relationship between classes of stone (here simply taken as M_{85}/M_{15} and D_{85}/D_{15}).

Further details of recommended methods of specifying gradings and of suggested gradings are given in the CUR/CIRIA Manual (1991), Subsec. 3.2.2.4.

Table 3. Examples of gradings.

Narrow grading $D_{85}/D_{15} < 1.5$		Wide grading $1.5 < D_{85}/D_{15} < 2.5$		Very wide grading $D_{85}/D_{15} > 2.5$	
Class	D_{85}/D_{15}	Class	D_{85}/D_{15}	Class	D_{85}/D_{15}
15–20t	1.10	1–9t	2.08	50–1000 kg	2.71
10–15t	1.14	1–6t	1.82	20–1000 kg	3.68
5–10t	1.26	100–1000 kg	2.15	10–1000 kg	4.64
3-7t	1.33	100–500 kg	1.71	10–500 kg	3.68
1–3t	1.44	10–80 kg	2.00	10–300 kg	3.10
300–1000 kg	1.49	10–60 kg	1.82	20–300 kg	2.46

2.3.3. *Structural parameters related to the cross-section*

There are many parameters related to the cross-section and most of them are obvious. Figure 5 gives an overview. The parameters are:

Crest freeboard, relative to still water level	R_c
Armor crest freeboard relative to swl	A_c
Difference between crown wall and armor crest	F_c
Armor crest level relative to the seabed	h_c
Structure width	B
Width of armor berm at crest	G_c
Thickness of armor, underlayer, filter	t_a, t_u, t_f
Area porosity	n_a
Angle of structure slope	α
Depth of the toe below still-water level	h_t

The permeability of the structure has an influence on the stability of the armor layer. This depends on the size of filter layers and core and can be given by a notional permeability factor, P. Examples of P are shown in Fig. 6, based on the work of Van der Meer (1988a).

The lower limit of P is an armor layer with a thickness of two diameters on an impermeable core (sand or clay) and with only a thin filter layer. This lower boundary is given by $P = 0.1$. The upper limit of P is given by a homogeneous structure which consists only of armor stones. In that case, $P = 0.6$. Two other values are shown in Fig. 6 and each particular structure should be compared with the given structures in order to make an estimation of the P factor. It should be noted that P is not a measure of porosity!

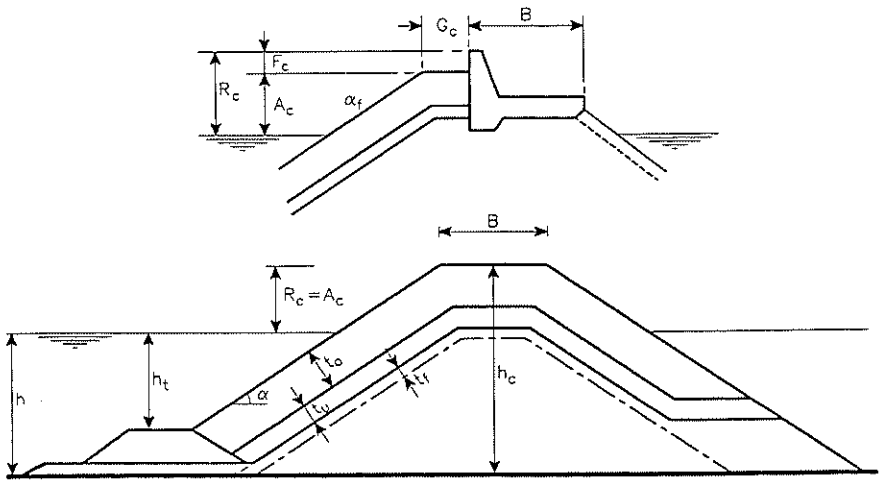

Fig. 5. Governing parameters related to the cross-section.

The estimation of P from Fig. 6 for a particular structure must, more or less, be based on engineering judgement. Although the exact value may not precisely be determined, a variation of P around the estimated value may well give an idea about the importance of the permeability.

The permeability factor P can also be determined by using a numerical (pc)-model that can give the volume of water that penetrates through the armor layer during run-up. Calculations should be done for the structures with $P = 0.5$ and 0.6 (see Fig. 6) and for the actual structure. As $P = 0.1$ gives no penetration at all, a graph can be made with P versus penetrated volume of water. The calculated volume for the actual structure then gives in the graph the P-value. The procedure has been described in more detail in Van der Meer (1988a).

With numerical models developed by Kobayashi and Wurjanto (1989, 1990), Van Gent (1993), or Engering *et al.* (1993), the penetration of water during run-up can be calculated fairly easy.

2.3.4. *Structural parameters related to the response of the structure*

The behaviour of the structure can be described by a few parameters. Statically

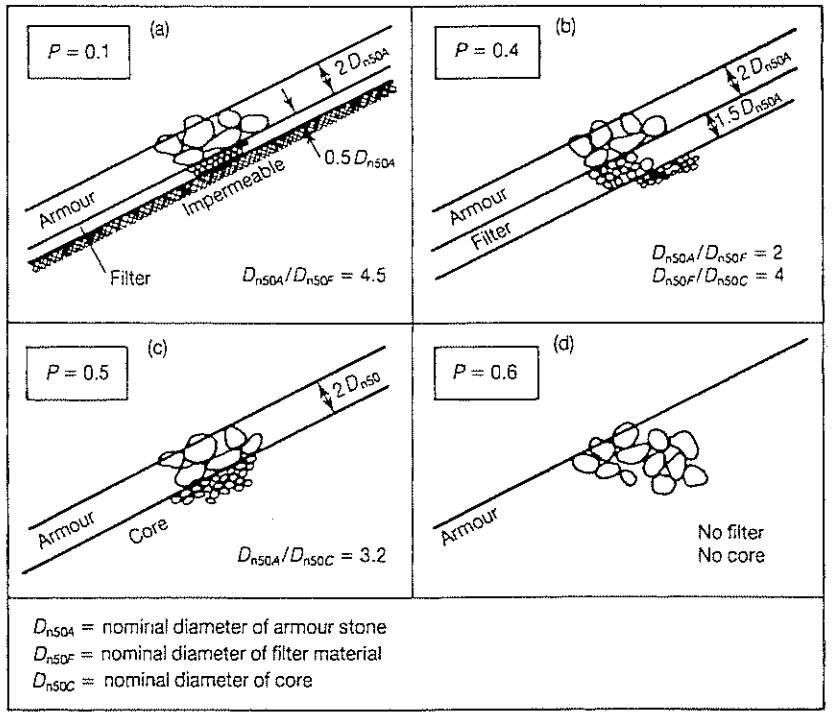

Fig. 6. Notional permeability factor P for various structures.

stable structures are described by the development of damage. This can be the amount of rock that is displaced or the displaced distance of a crown wall. Dynamically stable structures are described by a developed profile.

The damage to the armor layer can be given as a percentage of displaced stones related to a certain area (the whole or a part of the layer). In this case, however, it is difficult to compare various structures as the damage figures are related to different totals for each structure. Another possibility is to describe the damage by the erosion area around still-water level. When this erosion area is related to the size of the stones, a dimensionless damage level is presented which is independent of the size (slope angle and height) of the structure. This damage level is defined by

$$S = \frac{A_e}{D_{n50}^2} \tag{10}$$

where,

S = damage level,

A_e = erosion area around still-water level.

A plot of a structure with damage is shown in Fig. 7, the damage level taking both settlement and displacement into account. A physical description of the damage, S, is the number of squares with a side D_{n50} which fit into the erosion area. Another description of S is the number of cubic stones with a side of D_{n50} eroded within a D_{n50} wide strip of the structure. The actual number of stones eroded within this strip can be more or less than S, depending on the porosity, the grading of the armor stones and the shape of the stones. Generally, the actual number of stones eroded in a D_{n50} wide strip is equal to 0.7 to 1 times the damage S.

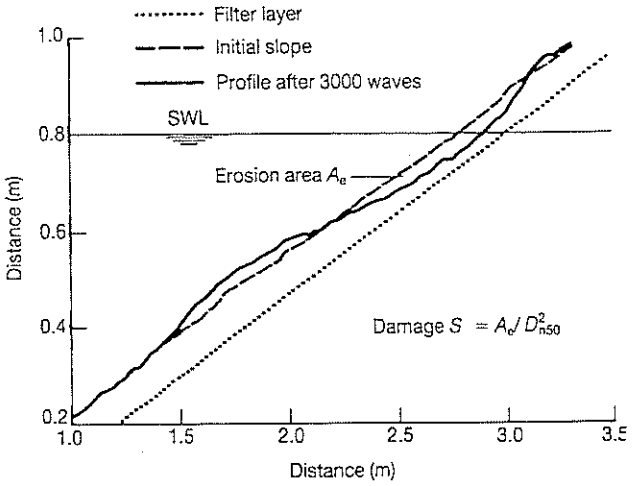

Fig. 7. Damage S based on erosion area A_e.

The limits of S depend mainly on the slope angle of the structure. For a two diameter thick armor layer, the values in Table 4 can be used. The initial damage of S = 2–3 is according to the criterion of the Hudson formula which gives 0–5% damage. Failure is defined as exposure of the filter layer. For S values higher than 15–20, the deformation of the structure results in an S-shaped profile and should be called dynamically stable.

Another definition is suggested for damage to concrete armor units. Such damage can be defined as the relative damage, N_o, which is the actual number of units (displaced, rocking, etc.) related to a width (along the longitudinal axis of the structure) of one nominal diameter, D_n. For cubes, D_n is the side of the cube; for tetrapods, $D_n = 0.65\ D$, where D is the height of the unit; for accropode, $D_n = 0.7D$; and for Dolosse, $D_n = 0.54\ D$ (with a waist ratio of 0.32).

Table 4. Design values of S for a two diameter thick armor layer.

Slope	Initial damage	Intermediate damage	Failure
1:1.5	2	3–5	8
1:2	2	4–6	8
1:3	2	6–9	12
1:4	3	8–12	17
1:6	3	8–12	17

An extension of the subscript in N_o can give the distinction between units displaced out of the layer, units rocking within the layer (only once or more times), etc. In fact the designer can define his own damage description, but the actual number is related to a width of one D_n. The following damage descriptions will be used in this paper:

N_{od} = units displaced out of the armor layer (hydraulic damage),

N_{or} = rocking units,

N_{omov} = moving units, $N_{omov} = N_{od} + N_{or}$.

The definition of N_{od} is comparable with the definition of S, although S includes displacement and settlement, but does not take into account the porosity of the armor layer. Generally, S is about twice N_{od}.

Dynamically stable structures are those where profile development is accepted. Units (stones, gravel, or sand) are displaced by wave action until a profile is reached where the transport capacity along the profile is reduced to a minimum. Dynamic stability is characterised by the design parameter profile.

An example of a schematised profile is shown in Fig. 8. The initial slope was 1:5 which is relatively gentle and one should note that Fig. 8 is shown on a distorted scale. The profile consists of a beach crest (the highest point of the profile), a curved slope around still-water level (above still-water level

steep, below gentle), and a steeper part relatively deep, below still-water level. For gentle slopes (shingle slope > 1:4), a step is found at this deep part. The profile is characterised by a number of lengths, heights, and angles and these were related to the wave boundary conditions and structural parameters (Van der Meer, 1988a).

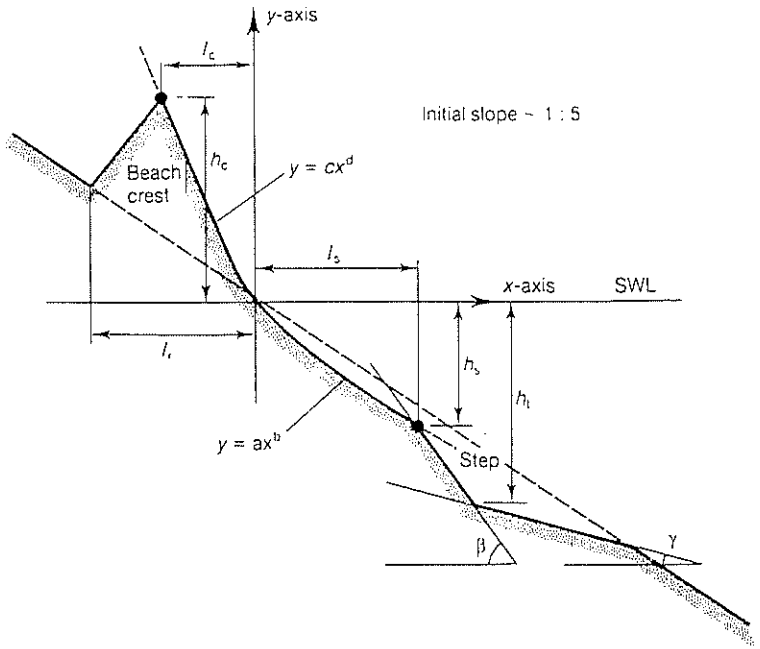

Fig. 8. Schematised profile on a 1:5 initial slope.

3. Hydraulic Response

This section presents methods that may be used for the calculation of the hydraulic response parameters which were also given in Fig. 3:

- run-up and run-down levels;
- overtopping discharges;
- wave transmission; and
- wave reflections.

Where possible, the prediction methods are identified with the limits of their application. These methods are generally available to describe the hydraulic response for only a few simplified cases, either because tests have been conducted for a limited range of wave conditions or because the structure geometry tested often represents a simplification in relation to many practical structures. It will therefore be necessary to estimate the performance for real situations from predictions for related (but dissimilar) structure configurations. Where this is not possible, or the predictions are less reliable than expected, physical model tests should be conducted.

3.1. *Wave run-up and run-down*

Predictions of R_u and R_d may be based on simple empirical equations, supported by model test results, or on numerical models of wave/structure interaction. One-dimensional numerical models of wave run-up have been developed by Kobayshi and Wurjanto (1989, 1990), Van Gent (1993), and Engering *et al.* (1993). A two-dimensional model has been developed by Van der Meer *et al.* (1992). These numerical models will not be discussed here.

All calculation methods require parameters to be defined precisely. Run-up and run-down levels are defined relative to still-water level (see Fig. 3). On some bermed and shallow slopes, run-down levels may not fall below still-water. All run-down levels in this paper are given as positive if below still-water level, and all run-up levels will also be given as positive if above it.

The upward excursion is generally greater than the downward, and the mean water level on the slope is often above still-water level. Again this may be most marked on bermed and shallow slopes. These effects often complicate the definition, calculation, or measurement of run-down parameters.

Much of the field data available on wave run-up and run-down apply to gentle and smooth slopes. Some laboratory measurements have been made on steeper smooth slopes and on porous armored slopes. Prediction methods for smooth slopes may be used directly for armored slopes that are filled or fully grouted with concrete or bitumen. These methods can also be used for rough nonporous slopes with an appropriate reduction factor.

The behaviour of waves on rough porous (rubble mound) slopes is very different from that on nonporous slopes, and the run-up performance is not well predicted by adapting equations for smooth slopes. Different data must be used. This difference is illustrated in Fig. 9, where significant relative run-up, R_{us}/H_s, is plotted for both smooth and rock slopes. The greatest divergence between the performance of the different slope types is seen for $1 < \xi_p < 5$. For ξ_p above 6 or 7, the run-up performance of smooth and porous slopes tends

to be very similar values. In that case, the wave motion is surging up and down the slope without breaking, and the roughness and porosity is then less important.

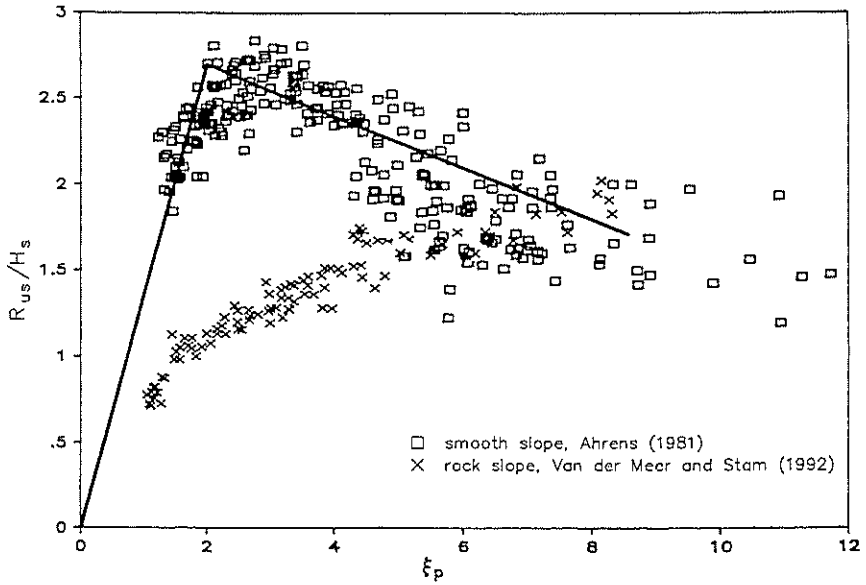

Fig. 9. Comparison of relative significant run-up for smooth and rubble mound slopes.

Delft Hydraulics has recently performed various applied fundamental research studies in physical scale models on wave run-up and overtopping on various structures (De Waal and Van der Meer, 1992). Run-up has extensively been measured on rock slopes. The influence on run-up and overtopping of berms, roughness on the slope (also one layer of rock) and shallow water, has been measured for smooth slopes. Finally, the influence of short-crested waves and oblique (long- and short-crested) waves has been studied on wave run-up and overtopping. All research was commissioned by the Technical Advisory Committee for Water Defenses (TAW) in The Netherlands. De Waal and Van der Meer (1992) give an overall view of the final results, such as design formulas and design graphs. Only the main results will be summarized here, then run-up and run-down on rock slopes will be dealt with.

A general run-up formula can be given with a smooth slope as a basis. This

formula for the 2% relative run-up $R_{u2\%}$ is given by

$$\frac{R_{u2\%}}{H_s} = 1.5\gamma\xi_p \text{ with a maximum of } 3.0\ \gamma \tag{11}$$

where H_s = the significant wave height, γ = a total reduction factor for various influences, and ξ_p = the surf similarity parameter based on the peak period. This general formula is shown in Fig. 10.

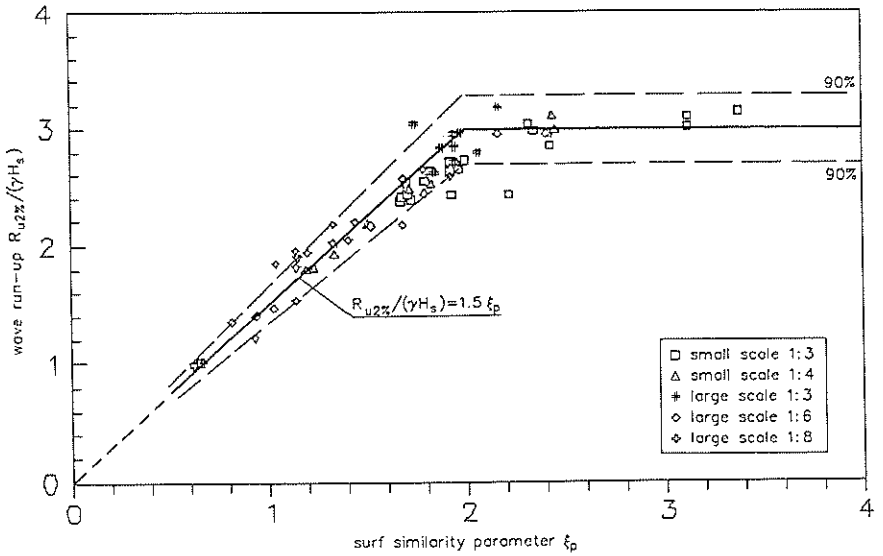

Fig. 10. General formula for wave run-up on a smooth slope, including various effects.

The influence of berms, roughness, shallow water, and oblique wave attack on wave run-up and overtopping can be given as reduction factors γ_b, γ_f, γ_h, and γ_β, respectively. They are defined as the ratio of run-up on a slope considered to that on a smooth impermeable slope under otherwise identical conditions (TAW, 1974). The total reduction factor then becomes

$$\gamma = \gamma_b\gamma_f\gamma_h\gamma_\beta. \tag{12}$$

For the reduction factors one is referred to De Waal and Van der Meer (1992). An overview of Eq. (12) with all test results is given in Fig. 11. In this figure, the vertical axis gives the relative run-up, divided by the total reduction

factor. Equation (11) can be considered as the average of the data (except for a small overprediction around $\xi_p = 2$). The reliability of the equation can be described by assuming the factor 1.5 as a stochastic variable with a normal distribution with mean 1.5 and variation coefficient (standard deviation divided by mean) of 0.085. The 90% confidence bands, for instance, can then be calculated by using 1.5 + 1.64*0.085 = 1.64 and 1.5 − 1.64*0.085 = 1.36 in Eq. (11). These bands are also shown in Fig. 11.

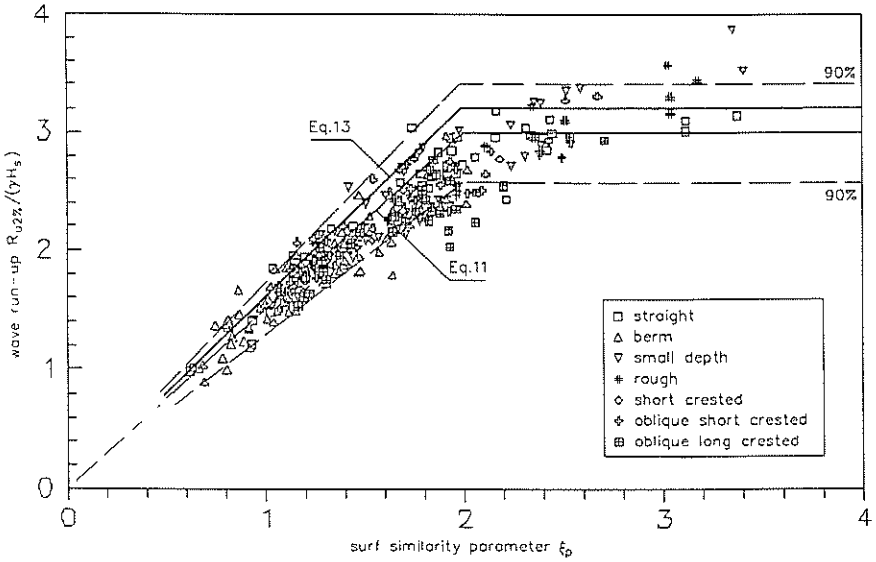

Fig. 11. Summary of test results for various structures and influences.

In a probabilistic design method, one can use Eq. (11) with the given variation coefficient. For a guideline, it is often a practice to include some safety in a formula, say, about one standard deviation. Therefore, the (deterministic) design formula used in The Netherlands is not Eq. (11), but

$$\frac{R_{u2\%}}{H_s} = 1.6\gamma\xi_p \text{ with a maximum of } 3.2\ \gamma. \tag{13}$$

Run-up levels on rubble slopes armored with rock armor or rip-rap have been measured in laboratory tests. In many instances, the rubble core has been reproduced as fairly permeable, except for those particular cases where an

impermeable core has been used. Therefore, test results often span a range within which the designer must interpolate.

Analysis of test data from measurements by Van der Meer and Stam (1992) has given prediction formulas for rock slopes with an impermeable core, described by a notional permeability factor $P = 0.1$, and porous mounds of relatively high permeability given by $P = 0.4 - 0.6$. The notional permeability factor P was described in Subsec. 2.3.3, Fig. 6.

Two sets of empirically derived formulas can be given for a run-up on rock slopes. The first set gives the run-up as a function of the surf similarity or breaker parameter. Coefficients for various run-up levels were derived. Secondly, the run-up was described as a Weibull distribution, including all possible run-up levels.

The prediction formulas for run-up versus surf similarity parameters are

$$\frac{R_{ux}}{H_s} = a\xi_m \text{ for } \xi_m < 1.5 \tag{14}$$

$$\frac{R_{ux}}{H_s} = b\xi_m^c \text{ for } \xi_m > 1.5\ . \tag{15}$$

The run-up for permeable structures ($P > 0.4$) is limited to a maximum:

$$\frac{R_{ux}}{H_s} = d\ . \tag{16}$$

In the above equations, coefficients are given in Table 5. Values for the coefficients a, b, c, and d have been determined for levels of $i = 0.1\%, 1\%, 2\%, 5\%$, 10%, significant, and mean run-up levels.

Table 5. Coefficients in run-up Eqs. (14)–(16) for rock slopes.

Run-up level	a	b	c	d
0.1%	1.12	1.34	0.55	2.58
1%	1.01	1.24	0.48	2.15
2%	0.96	1.17	0.46	1.97
5%	0.86	1.05	0.44	1.68
10%	0.77	0.94	0.42	1.45
sign.	0.72	0.88	0.41	1.35
mean	0.47	0.60	0.34	0.82

Results of the tests and the equations are shown, for example, values of $i = 2\%$, and significant, for each of $P = 0.1$ and $P > 0.4$, in Figs. 12 and 13.

The reliability of Eqs. (14)–(16) can be described by assuming coefficients a, b, and d as stochastic variables with a normal distribution. The variation coefficients for these coefficients are 7% for $P < 0.4$ and 12% for $P \geq 0.4$. Confidence bands can be calculated based on these variation coefficients.

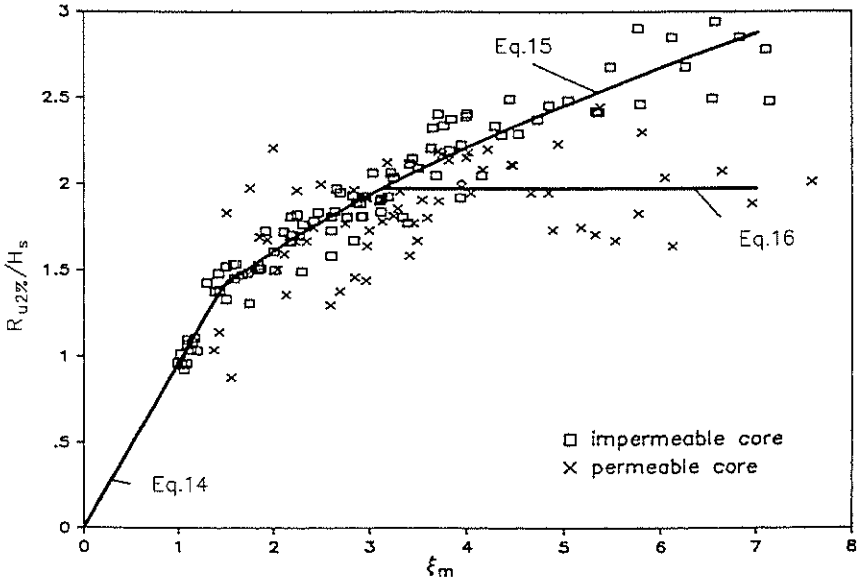

Fig. 12. Relative 2% run-up on rock slopes.

The second method is to describe the run-up as a Weibull distribution:

$$p = P\{R_u > R_{up}\} = e^{-(\frac{R_{up}}{b})^c} \tag{17}$$

or

$$R_{up} = b(-\ln p)^{\frac{1}{c}} \tag{18}$$

where,

p = probability (between 0 and 1),

R_{up} = run-up level exceeded by p * 100% of the run-up levels,

b = scale parameter,

c = shape parameter.

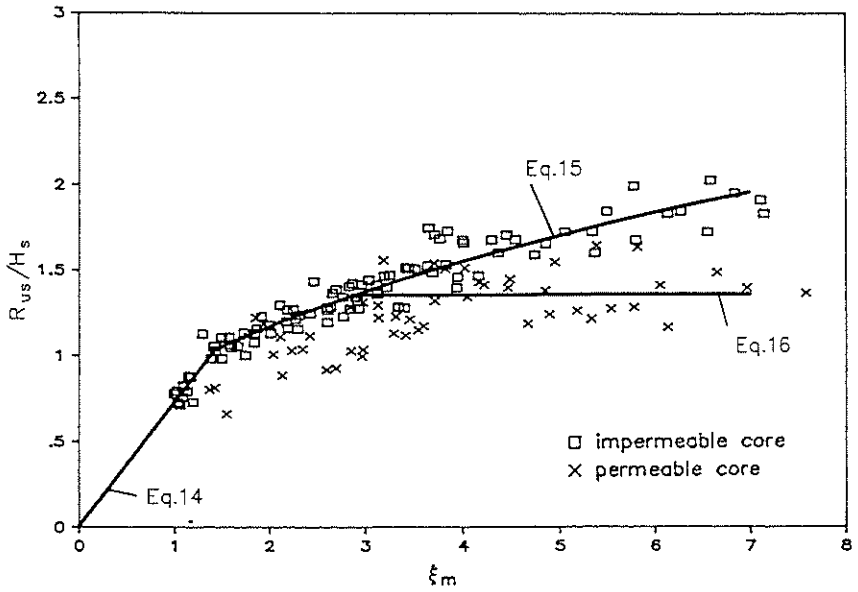

Fig. 13. Relative significant run-up on rock slopes.

The shape parameter c defines the shape of the curve. For $c = 2$, a Rayleigh distribution is obtained. The scale parameter can be described by,

$$\frac{b}{H_s} = 0.4 s_{om}^{-0.25} \cot\alpha^{-0.2}. \tag{19}$$

The shape parameter is described by,

a. for plunging waves:

$$c = 3.0 \xi_m^{-0.75}, \tag{20}$$

b. for surging waves,

$$c = 0.52 P^{-0.3} \xi_m^P \sqrt{\cot\alpha}\,. \tag{21}$$

The transition between Eqs. (20) and (21) is described by a critical value for the surf similarity parameter, ξ_{mc},

$$\xi_{mc} = [5.77 P^{0.3} \sqrt{\tan\alpha}]^{\frac{1}{P+0.75}} \tag{22}$$

For $\xi_m < \xi_{mc}$, Eq. (20) should be used and for $\xi_m > \xi_{mc}$, Eq. (21). The formulas are only applicable for slopes with $\cot\alpha \leq 2$. For steeper slopes the distributions on a 1:2 slope may give a first estimation.

Examples of run-up distributions are shown in Fig. 14. The reliability of Eqs. (20)–(22) can be described by assuming b as a stochastic variable with a normal distribution. The variation coefficient of b is 6% for $P < 0.4$ and 9% for $P \geq 0.4$. Confidence bands can be calculated by means of these variation coefficients.

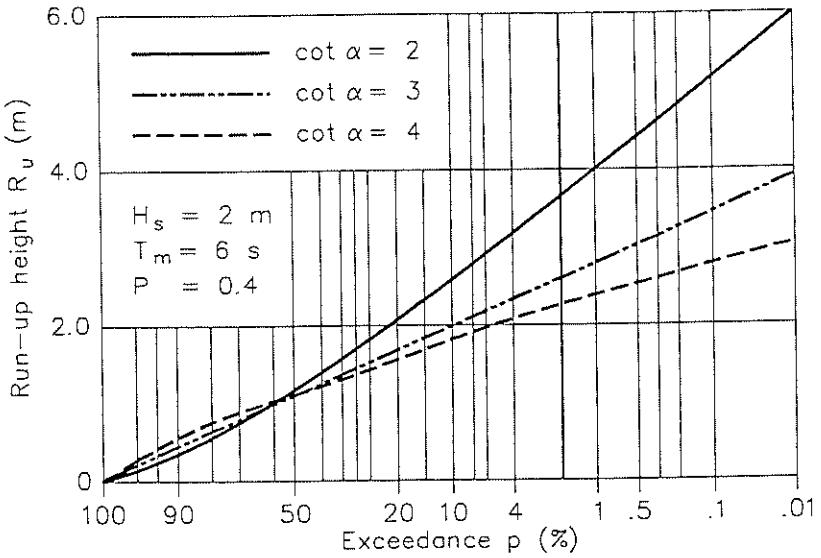

Fig. 14. Run-up distributions on a rock slope.

Run-down levels on porous rubble slopes are also influenced by the permeability of the structure, and by the surf similarity parameter. Analysis of the 2% run-down level on the sections tested by Van der Meer (1988a) has given an equation which includes the effects of structure permeability and wave steepness:

$$\frac{R_{d2\%}}{H_s} = 2.1\sqrt{\tan\alpha} - 1.2P^{0.15} + 1.5e^{-60s_{om}}. \qquad (23)$$

Test results are shown in Fig. 15 for an impermeable and a permeable core. The presentation with ξ_m only gives a large scatter. Including the slope angle and the wave steepness separately and also the permeability as in Eq. (23) reduces the scatter considerably.

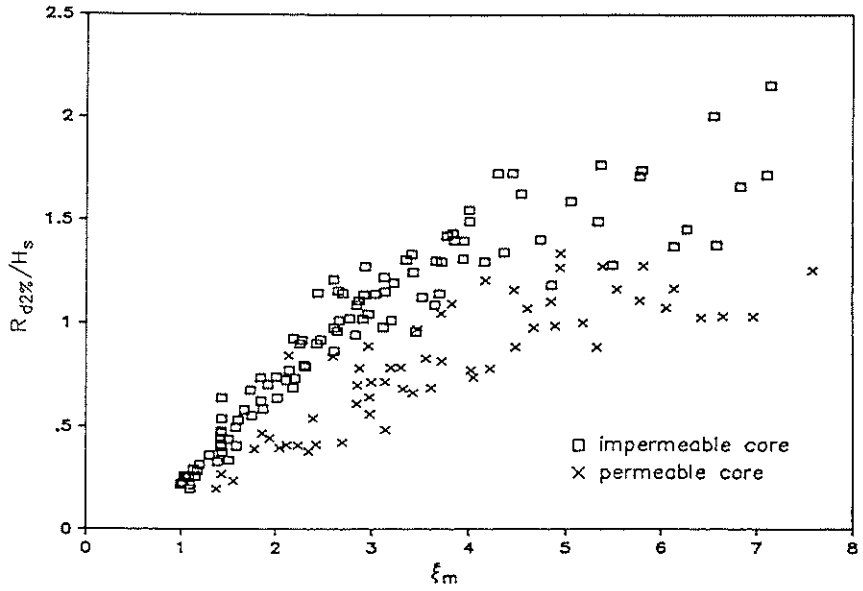

Fig. 15. Run-down $R_{d2\%}/H_s$ on impermeable and permeable rock slopes.

3.2. *Overtopping*

In the design of many sea walls and breakwaters, the controlling hydraulic response is often the wave overtopping discharge. Under random waves this varies greatly from one wave to another. There are some data available to quantify this variation. For many cases it is sufficient to use the mean discharge, q, usually expressed as a discharge per metre run (m^3/s per m).

Suggested critical values of q for various design situations are summarised in Fig. 16. This incorporates recommended limiting values of the mean discharge for the stability of crest and rear armor to types of seawalls and/or the safety of vehicles and people. Most data in Fig. 16 refer to old Japanese data. De Gerloni *et al.* (1991) and Franco (1993) investigated critical overtopping discharges at vertical breakwaters for (model) cars and people (model and prototype). Their results give larger allowable overtopping (see Fig. 16). Dutch results in Delft Hydraulics' large Deltaflume on a prototype grass dike showed that situations with overtopping more than 1–5 l/s per meter were not accessible anymore for people by foot. This situation is also given in Fig. 16.

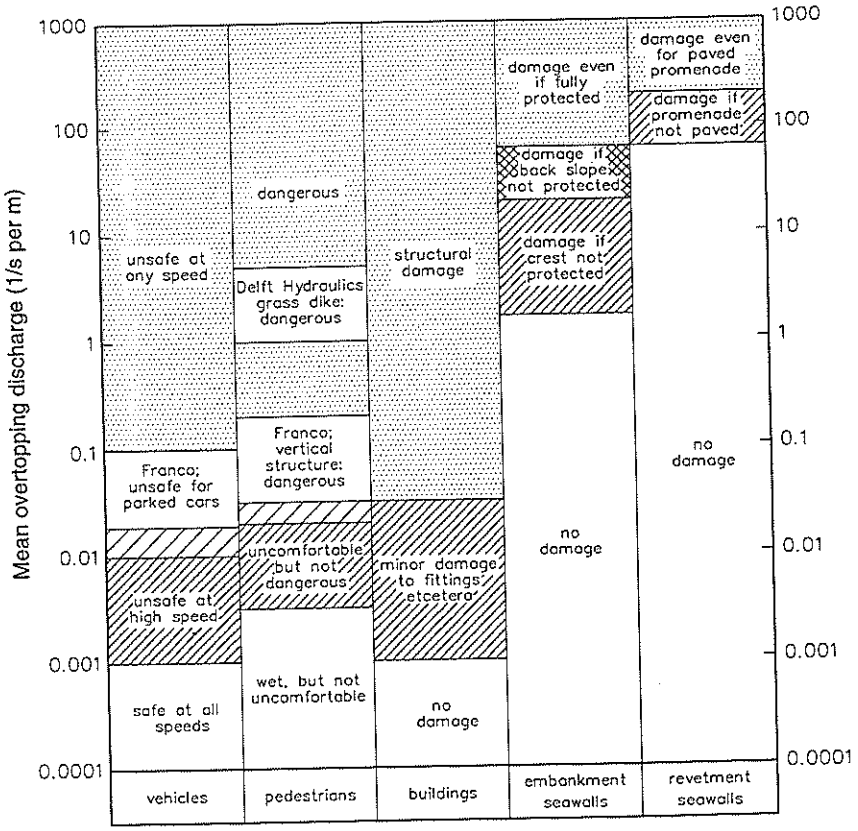

Fig. 16. Critical overtopping discharges.

The calculation of overtopping discharge for a particular structure geometry, water level, and wave condition is based on empirical equations fitted to hydraulic model test results. The data available on overtopping performance is restricted to a few structural geometries. A well-known and wide data set applies to plain and bermed smooth slopes without crown walls (Owen, 1980). More restricted studies have been reported by TAW (1974), Bradbury *et al.* (1988), and Aminthi and Franco (1988). Recently, Delft Hydraulics finished two extensive studies on wave run-up and overtopping (De Waal and Van der Meer, 1992).

Each of these studies have developed dimensionless parameters of the crest freeboard for use in prediction formulas. Different dimensionless groups have

been used by each author. The simplest of such parameters is the relative freeboard, R_c/H_s. This simple parameter, however, omits the important effects of the wave period or wave steepness and slope angle.

For plain and bermed smooth slopes, Owen (1980) relates a dimensionless discharge parameter, Q, to a dimensionless freeboard parameter, R, by an exponential equation of the form

$$Q = ae^{-bR/\gamma}. \tag{24}$$

The definitions of Q and R that were given by Owen (1980) are

$$Q = \frac{q}{\sqrt{gH_s^3}}\sqrt{\frac{s_{om}}{2\pi}} \tag{25}$$

$$R = \frac{R_c}{H_s}\sqrt{\frac{s_{om}}{2\pi}} \tag{26}$$

and values for the coefficients a and b were derived from the test results and are given in Table 6.

Table 6. Values of the coefficients a and b in Eq. (24) for straight smooth slopes. (Owen, 1980).

slope	a	b
1:1	0.00794	20.12
1:1.5	0.0102	20.12
1:2	0.0125	22.06
1:3	0.0163	31.9
1:4	0.0192	46.96
1:5	0.025	65.2

De Waal and Van der Meer (1992) used Owen's data on smooth slopes and also data from Führböter *et al.* (1989), besides their own extensive measurements (see Subsec. 3.1). They derived two approaches, one by relating overtopping to wave run-up and the other by treating overtopping separately. Both methods are given here.

The simplest approach for determining wave overtopping is followed when the crest freeboard R_c is related to an expected run-up level on a nonovertopped slope, say, the $R_{u2\%}$. This "shortage in run-up height" can then be

described by $(R_{u2\%} - R_c)/H_s$. Equations (11) and (12) can be used to determine $R_{u2\%}$, including all influences of berms, etc. (see Subsec. 3.1). For rock slopes, Eqs. (14) to (20) can be used.

The simplest dimensionless description of overtopping is given by Eq. (3). Figure 17 shows the final results on overtopping and gives all available data, including data of Owen (1980), Führböter *et al.* (1989), and various tests at Delft Hydraulics. The horizontal axis gives the "shortage in run-up height" $(R_{u2\%} - R_c)/H_s$. For the zero value, the crest height is equal to the 2% run-up height. For negative values, the crest height is even higher and overtopping will be (very) small. For a value of 1.5, the crest level is 1.5 H_s lower than the 2% run-up height and overtopping will obviously be large. The vertical axis gives the logarithmic of the mean dimensionless overtopping discharge Q.

Figure 17 gives about 500 data points. The formula that describes more or less the average of the data is given by an exponential function as suggested by Owen (1980):

$$Q = \frac{q}{\sqrt{gH_s^3}} = 8.10^{-5} e^{3.1 \frac{(R_{u2\%} - R_c)}{H_s}} \tag{27}$$

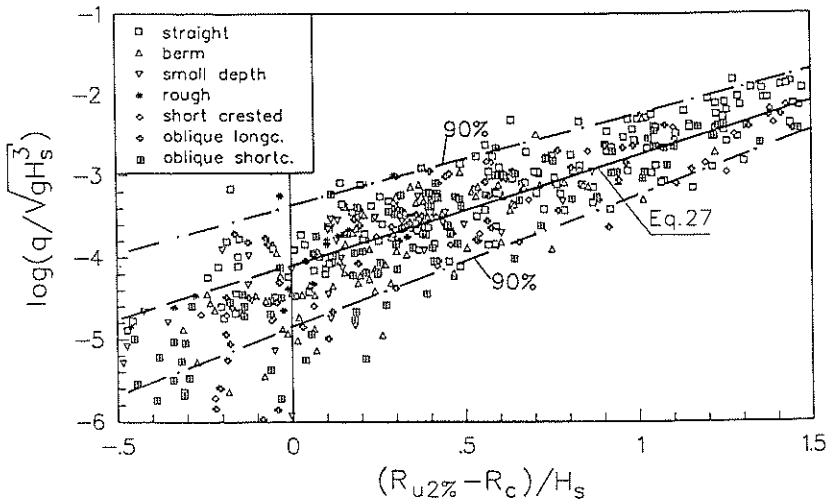

Fig. 17. Wave overtopping on slopes as a function of wave run-up.

The reliability of Eq. (27) can be given by assuming that $\log Q$ (and not Q) has a normal distribution with a variation coefficient $V = \sigma/\mu = 0.11$.

Reliability bands can then be calculated for various practical values of mean overtopping discharges.

The approach described above has a limited application if the overtopping volume becomes fairly large, or if the crest height is much lower than the 2% run-up height, especially when reduction factors for influences of berms, etc., are applied. In those cases above, the method should be applied with care and the method described below is preferred.

From the analysis of De Waal and Van der Meer (1992), it was found that wave overtopping should be divided into situations with plunging and with surging waves. In fact, this corresponds with wave run-up (see Figs. 10 and 11). The dimensionless overtopping discharge is given by Q_b and Q_n, and the dimensionless crest height by R_b and R_n, respectively, where the index b means breaking (plunging, $\xi_p < 2$) waves and n means nonbreaking (surging, $\xi_p > 2$) waves. The definitions are

$$Q_b = \frac{q}{\sqrt{gH_s^3}} \sqrt{\frac{s_{op}}{\tan\alpha}}\,, \tag{28}$$

$$R_b = \frac{R_c}{H_s} \frac{\sqrt{s_{op}}}{\tan\alpha} \frac{1}{\gamma}\,, \tag{29}$$

$$Q_n = \frac{q}{\sqrt{gH_s^3}}\,, \tag{30}$$

$$R_n = \frac{R_c}{H_s} \frac{1}{\gamma}\,. \tag{31}$$

The total reduction factor γ is described in Subsec. 3.1.

The average of all data for breaking waves is shown in Fig. 18 and can be described again by an exponential function:

$$Q_b = 0.06 e^{-5.2 R_b}. \tag{32}$$

The reliability of Eq. (32) can be given by assuming the coefficient 5.2 to be a stochastic variable with normal distribution with mean 5.2 and standard deviation 0.55.

A similar graph is shown in Fig. 19 for nonbreaking waves and the average of the data can be described by

$$Q_n = 0.2 e^{-2.6 R_n}. \tag{33}$$

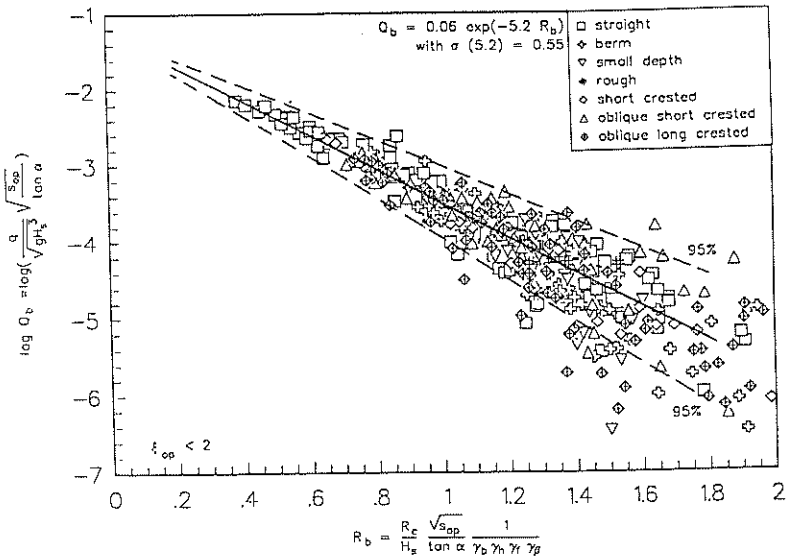

Fig. 18. Wave overtopping for breaking (plunging) waves, $\xi_p < 2$.

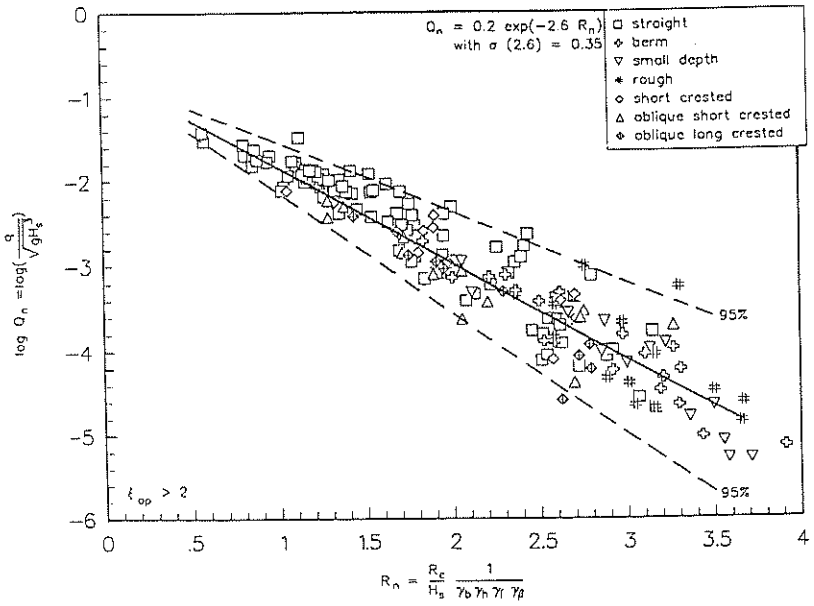

Fig. 19. Wave overtopping for nonbreaking (surging) waves, $\xi_p > 2$.

The reliability can now be described by a standard deviation of 0.35 for the coefficient 2.6.

Surprisingly, there are very little data available describing the overtopping performance of rock armored sea walls without crown walls. However, the results from two tests by Bradbury *et al.* (1988) may be used to give estimates of the influence of wave conditions and relative freeboard. Again the test results have been used to give values of coefficients in an empirical equation. Bradbury *et al.* give the following prediction formula:

$$Q = aR^{-b} \tag{34}$$

with

$$Q = \frac{Q}{\sqrt{gH_s^3}}\sqrt{\frac{s_{om}}{2\pi}}\,, \tag{35}$$

$$R = \left(\frac{R_c}{H_s}\right)^2\sqrt{\frac{s_{om}}{2\pi}}\,. \tag{36}$$

Values of a and b have been calculated from the results of tests with a rock armored slope at 1:2 with the crest details shown in Fig. 20. For section A, $a = 3.7{*}10^{-10}$ and $b = 2.92$. For section B, $a = 1.3{*}10^{-9}$ and $b = 3.82$.

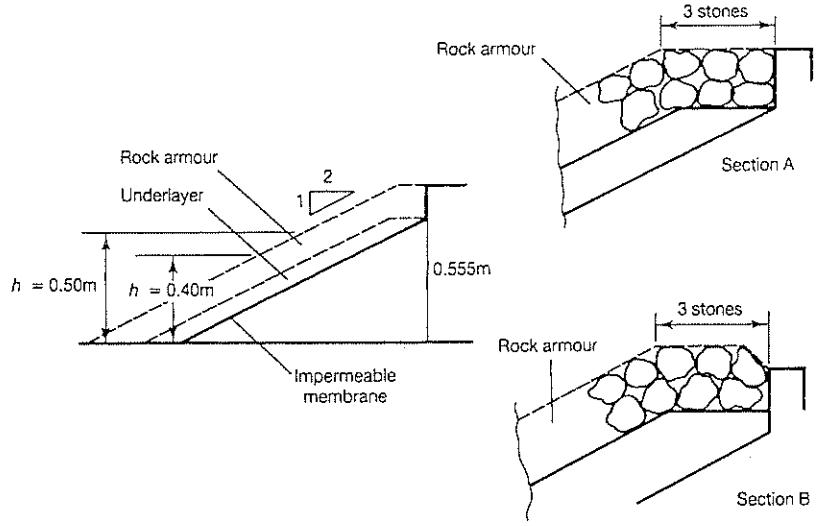

Fig. 20. Overtopped rock structures with low crown wall. (Bradbury *et al.*, 1988)

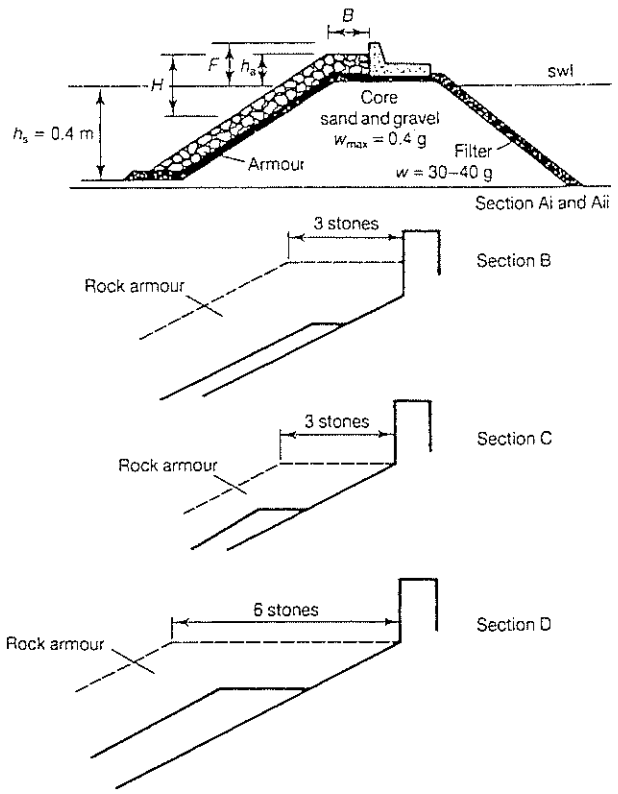

Fig. 21. Studies of tested cross-sections.

More data are available to describe the overtopping performance of rock armored structures with crown walls. Tests have been conducted by Bradbury *et al.* (1988) and Aminthi and Franco (1988), and the results have been used to determine values for coefficients a and b in Eq. (34). The cross-sections studied are illustrated in Fig. 21 and values for the coefficients are given in Table 7. Each of these studies have used different dimensionless freeboard and discharge parameters in empirical equations that are valid for a range of different structural configurations. The data have not been analysed as a single set, and the user may, therefore, need to compare the results given by more than one prediction method.

Table 7. Coefficients a and b in Eq. (34) for overtopping discharges over cross-sections in Fig. 21.

Section	Slope angle	B/H_s	a	b
Ai	1:2.0	1.10	1.7×10^{-8}	2.41
		1.85	1.8×10^{-7}	2.30
		2.60	2.3×10^{-8}	2.68
Aii	1:1.33	1.10	5.0×10^{-8}	3.10
		1.85	6.8×10^{-8}	2.65
		2.60	3.1×10^{-8}	2.69
B	1:2	0.79–1.7	1.6×10^{-9}	3.18
C	1:2	0.79–1.7	5.3×10^{-9}	3.51
D	1:2	1.6–3.3	1.0×10^{-9}	2.82

3.3. *Transmission*

Structures such as breakwaters constructed with low crest levels will transmit wave energy into the area behind the breakwater. The transmission performance of low-crested breakwaters is dependent on the structure geometry, principally, the crest freeboard, crest width and water depth, permeability, and on the wave conditions, principally, the wave height and period.

Hydraulic model test results measured by Seelig (1980), Powell and Allsop (1985), Daemrich and Kahle (1985), Ahrens (1987), and Van der Meer (1988a) have been reanalysed by Van der Meer (1990b) to give a single prediction method. This relates C_t to the relative crest freeboard, R_c/H_s. The data used are plotted in Fig. 22. The prediction equations describing the data may be summarised:

Range of validity	Equation	
$-2.0 < \frac{R_c}{H_s} < -1.13$	$C_t = 0.80$	(37)
$-1.13 < \frac{R_c}{H_s} < 1.2$	$C_t = 0.46 - 0.3\frac{R_c}{H_s}$	(38)
$1.2 < \frac{R_c}{H_s} < 2.0$	$C_t = 0.10$	(39)

Figure 22 shows all results together with the equations. These equations give a very simplistic description of the data available, but will often be sufficient for a preliminary estimate of performance. The upper and lower bounds

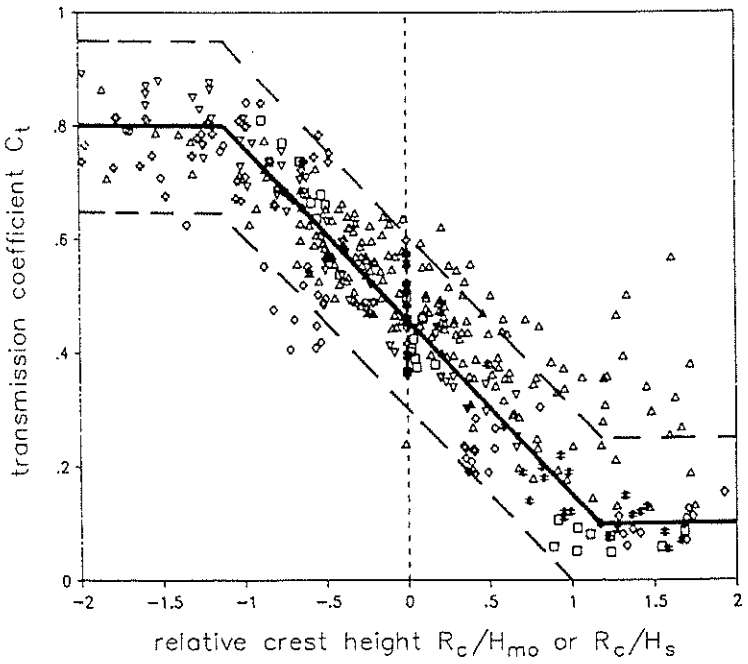

Fig. 22. Wave transmission over and through low-crested structures.

of the data considered are given by lines 0.15 higher (or lower) than the mean lines given above. This corresponds with the 90% confidence bands (the standard deviation was 0.09).

A second analysis on the data was performed by Daemen (1991) and he also performed more tests on wave transmission. A summary has been described by Van der Meer and d'Angremond (1991) and Van der Meer and Daemen (1994) and is given here.

Until now wave transmission has been described in the conventional way as a function of R_c/H_s. It is not clear, however, that the use of this combination of crest freeboard and wave height produces similar results with, on the one hand, constant R_c and variable H_s and, on the other, variable R_c and constant H_s. Moreover, when R_c becomes zero, all influence of the wave height is lost which leads to a large scatter in the graph at $R_c = 0$.

Therefore, it was decided to separate R_c and H_s in the second analysis.

The mass or nominal diameter of the armor layer of a rubble mound structure is determined by the extreme wave attack that can be expected during the lifetime of the structure. There is a direct relationship between the design wave height and the size of armor rock, which is often given as the stability factor $H_s/\Delta D_{n50}$, where Δ is the relative buoyant density. It can be concluded that the nominal diameter of the armor layer characterises the rubble mound structure. It is, therefore, also a good parameter to characterise both the wave height and the crest height in a dimensionless way.

The relative wave height can then be given as H_s/D_{n50}, in accordance with the stability factor, and the relative crest height by R_c/D_{n50}, being the number of rocks that the crest level is above or below still-water level.

Moreover, a separation into H_s/D_{n50} and R_c/D_{n50} enables a distinction between various cases. For example, low H_s/D_{n50} values (smaller than 1 to 2) produce low waves traveling through the crest and high H_s/D_{n50} values (3 to 5) yield situations under extreme wave attack. Finally, D_{n50} can be used to describe other breakwater properties as the crest width B. This yields the parameter B/D_{n50}.

The primary parameters for wave transmission can now be given as

Relative crest height:	R_c/D_{n50}
Relative wave height:	H_s/D_{n50}
Fictitious wave steepness:	s_{op}
And possibly:	B/D_{n50} .

The outcome of the analysis on wave transmission, including the data of Daemen (1991), was a linear relationship between the wave transmission coefficient C_t and the relative crest height R_c/D_{n50}, which is valid between minimum and maximum values of C_t. In Fig. 23, the basic graph is shown. The linearly increasing curves are presented by

$$C_t = a\frac{R_c}{D_{n50}} + b \tag{40}$$

with

$$a = 0.031\frac{H_i}{D_{n50}} - 0.24 \; . \tag{41}$$

Equation (41) is applicable for conventional and reef-type breakwaters. The coefficient "b" for conventional breakwaters is described by

$$b = -5.42 s_{op} + 0.0323\frac{H_i}{D_{n50}} - 0.0017\left(\frac{B}{D_{n50}}\right)^{1.84} + 0.51 \; , \tag{42}$$

and for reef-type breakwaters by

$$b = -2.6 s_{op} - 0.05 \frac{H_i}{D_{n50}} + 0.85 \,. \tag{43}$$

The following minimum and maximum values are derived:

Conventional breakwaters:
Minimum: $C_t = 0.075$; maximum: $C_t = 0.75$. (44)

Reef-type breakwaters:
Minimum: $C_t = 0.15$; maximum: $C_t = 0.60$
for $R_c/D_{n50} < -2$, linearly increasing to $C_t = 0.80$ for $R_c/D_{n50} = -6$. (45)

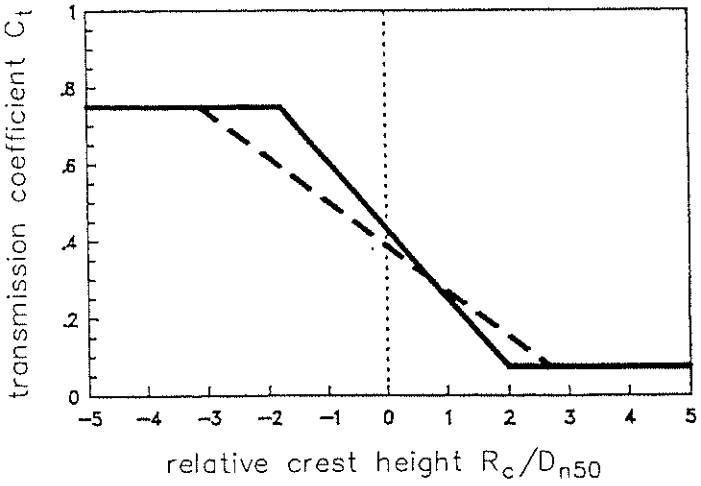

Fig. 23. Basic graph for wave transmission.

The analysis was based on various groups with constant wave steepness and a constant relative wave height. The validity of the wave transmission formula (Eq. 40) corresponds, of course, with the ranges of these groups that were used. The formula is valid for

$$1 < H_s/D_{n50} < 6 \text{ and } 0.01 < s_{op} < 0.05 \,.$$

Both upper boundaries can be regarded as physically bound. Values of $H_s/D_{n50} > 6$ will cause instability of the structure and values of $s_{op} > 0.05$ will cause waves breaking on steepness. In fact, boundaries are only given for extremely low wave heights relative to the rock diameter and for very low wave steepnesses (low swell waves).

The formula is applicable outside the range given above, but the reliability is low. Figure 24 shows the measured wave transmission coefficient versus the calculated one from Eq. (40) for various data sets of conventional breakwaters. The reliability of the formula can be described by assuming a normal distribution around the line in Fig. 24. With the restriction of the range of application given above, the standard deviation amounted to $\sigma(C_t) = 0.05$, which means that the 90% confidence levels can be given by $C_t \pm 0.08$. This is a remarkable increase in reliability compared to the simple formula given by Eqs. (37)–(39) and Fig. 22, where a standard deviation of $\sigma(C_t) = 0.09$ is given.

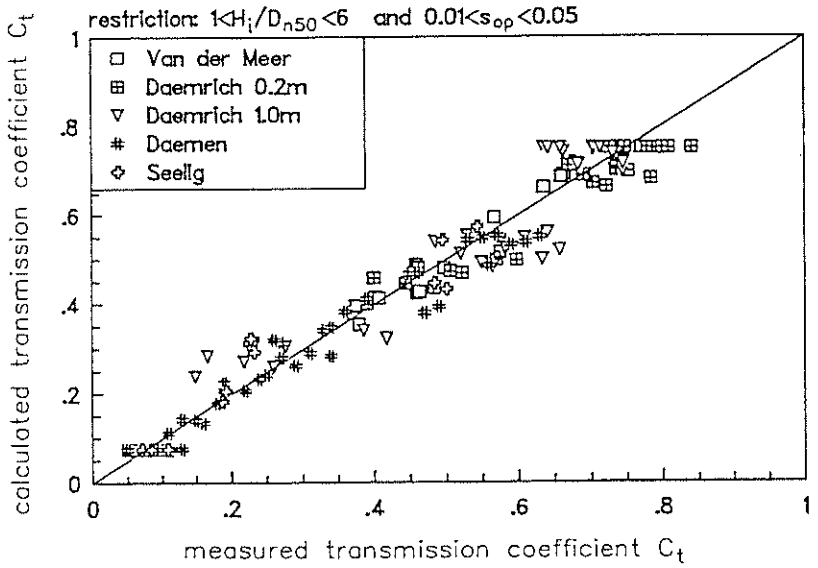

Fig. 24. Calculated (Eq. 40) versus measured wave transmission for conventional breakwaters.

The reliability of the formula for reef-type breakwaters is more difficult to describe. If only tests are taken where the crest height had been lowered to less than 10% of the initial height h_c', and the test conditions lie within the range of application, the standard deviation amounts to $\sigma(C_t) = 0.031$. If the

restriction on the crest height is not taken into account, the standard deviation amounts to $\sigma(C_t) = 0.054$.

3.4. *Reflections*

Waves will reflect from nearly all coastal or shoreline structures. For structures with nonporous and steep faces, approximately 100% of the wave energy incident upon the structure will reflect. Rubble slopes are often used in harbor and coastal engineering to absorb wave action. Such slopes will generally reflect significantly less wave energy than the equivalent nonporous or smooth slope. Although some of the flow processes are different, it has been found convenient to calculate the reflection performance given by C_r using an equation of the same form as for nonporous slopes, but with different values of the empirical coefficients to match the alternative construction. Data for random waves are available for smooth and armored slopes at angles between 1:1.5 and 1:2.5 (smooth), and 1:1.5 and 1:6 (rock).

Data by Allsop and Channell (1988) will be given here, together with data by Van der Meer (1988a), analysed by Postma (1989). Formulas of other references will be used for comparison.

For smooth impermeable slopes, Battjes (1974) gives

$$C_r = 0.1\xi^2 \,. \tag{46}$$

Seelig (1983) gives

$$C_r = \frac{a\xi_p^2}{b + \xi_p^2} \tag{47}$$

with
$a = 1.0, b = 5.5$ for smooth slopes,
$a = 0.6, b = 6.6$ for a conservative estimate of rough permeable slopes.

Equations (46) and (47) are shown in Fig. 25 together with the reflection data of Van der Meer (1988a) for rock slopes. The two curves for smooth slopes are close. The curve of Seelig (1983) for permeable slopes is not a conservative estimate, but it even underestimates the reflection for large ξ_p values.

The best fit curve through all the data points in Fig. 25 is given by Postma (1989) and is also given in the figure:

$$C_r = 0.14\,\xi_p^{0.73} \quad \text{with } \sigma(C_r) = 0.055 \,. \tag{48}$$

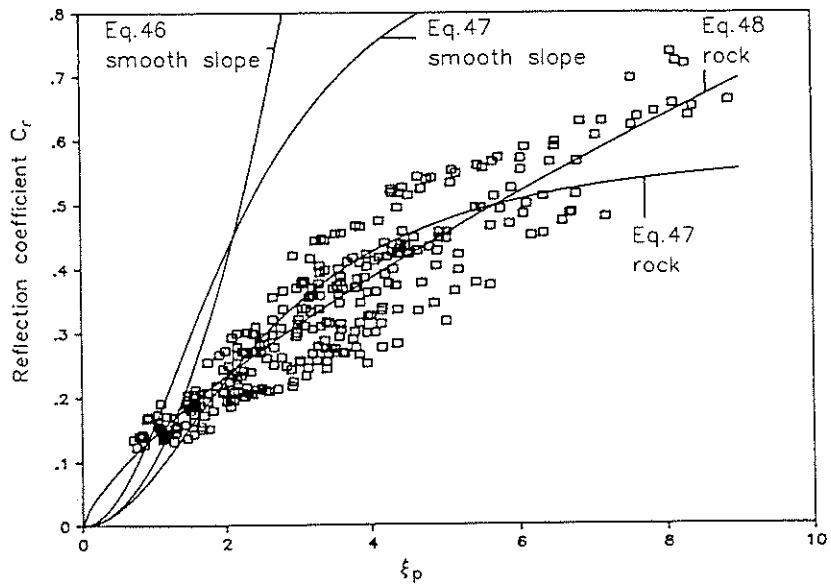

Fig. 25. Comparison of data on rock slopes with other formulas. (Van der Meer 1988a)

The surf similarity parameter did not describe the combined slope angle-wave steepness influence in a sufficient way. Therefore, both the slope angle and wave steepness were treated separately and Postma derived the following relationship

$$C_r = 0.071 P^{-0.082} \cot\alpha^{-0.62} s_{op}^{-0.46}, \tag{49}$$

with

$\sigma(C_r) = 0.036$,

P = notional permeability factor described in Subsec. 2.3.3.

The standard deviation of 0.055 in Eq. (48) reduced to 0.036 in Eq. (49) which is a considerable increase in reliability.

The results of random wave tests by Allsop and Channell (1989), analysed to give values for the coefficients a and b in Eq. (47) (but with ξ_m instead of ξ_p), is presented below. The rock armored slopes used rock in two or one layer, placed on an impermeable slope covered by underlayer stone, is equivalent to

$P = 0.1$. The range of wave conditions for which these results may be used is given by

$$0.004 < s_{om} < 0.052, \text{ and } 0.6 < H_s/\Delta D_{n50} < 1.9 .$$

Slope type	a in (47)	b in (47)
Smooth	0.96	4.80
Rock, two layers	0.64	8.85
Rock, one layer	0.64	7.22

Postma (1989) also reanalysed the data given by Allsop and Channell which were described above. Figure 26 gives the data by Allsop and Channell together with Eq. (48). The curve is a little higher than the average given in the data. The best fit curve is described by

$$C_r = 0.125\ \xi_p^{0.73} \qquad \text{with } \sigma(C_r) = 0.060 . \tag{50}$$

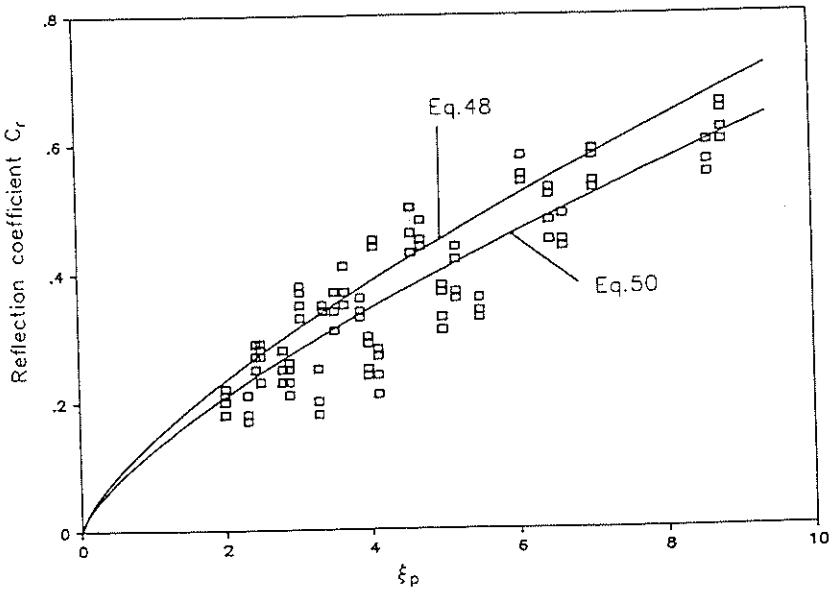

Fig. 26. Data of Allsop and Channell (1989).

4. Structural Response

4.1. *Introduction*

The hydraulic and structural parameters are described in Sec. 2 and the hydraulic responses in Sec. 3. Figure 3 gives an overview of the definitions of the hydraulic parameters and responses as wave run-up, run-down, overtopping, transmission, and reflection, and Fig. 5 shows the structural parameters which are related to the cross-section. The response of the structure under hydraulic loads will be described in this section and design tools will be given.

The design tools described here permit the design of many structure types. Nevertheless, it should be remembered that each design rule has its limitations. For each structure which is important and expensive to build, it is advised to perform physical model studies.

Figure 27 gives the same cross-section as in Fig. 5, but it now shows the various parts of the structure which will be described in the following sections. Some general points and design rules for the geometrical design of the cross-section will be given here. These are

- the minimum crest width,
- the thickness of (armor layers),
- the number of units or rocks per surface area,
- the bottom elevation of the armor layer.

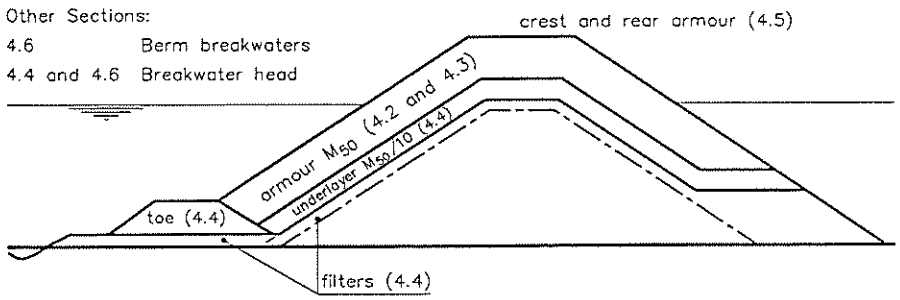

Fig. 27. Various parts of a structure.

The crest width is often determined by construction methods used (access on the core by trucks or crane) or by functional requirements (road/crown wall on the top). Where the width of the crest can be small, a required minimum

width $B_{\min}$ should be provided, where (SPM, 1984)

$$B_{\min} = (3 \text{ to } 4) D_{n50} \,. \tag{51}$$

The thickness of layers is given by

$$t_a = t_u = t_f = n\, k_t\, D_{n50} \,. \tag{52}$$

The number of units per m^2 is given by

$$N_a = n\, k_t (1 - n_v) D_{n50}^{-2} \,. \tag{53}$$

Where t_a, t_u, t_f = thickness of armor, underlayer, or filter,

n = number of layers,

k_t = layer thickness coefficients,

n_v = volumetric porosity.

Values of k_t and n_v as given in the SPM (1984) are

	k_t	n_v
Smooth rock, $n = 2$	1.02	0.38
Rough rock, $n = 2$	1.00	0.37
Rough rock, $n > 3$	1.00	0.40
Graded rock	–	0.37
Cubes	1.10	0.47
Tetrapods	1.04	0.50
Dolosse	0.94	0.56

Another source for values of k_t and n_v for rock is the CUR/CIRIA Manual (1991):

Shape of rock	Placement	k_t	n_v
Irregular	Random	0.75	0.40
Irregular	Special	1.05–1.20	0.39
Semi-round	Random	0.75	0.37
Semi-round	Special	1.10–1.25	0.36
Equant	Random	0.80	0.38
Equant	Special	1.00–1.15	0.37
Very round	Random	0.80	0.36
Very round	Special	1.05–1.20	0.35

The number of units in a rock layer depends on the grading of the rock. The values of k_t that are given above describe a rather narrow grading (uniform rock). For riprap and even wider graded material the number of stones can not easily be estimated. In that case, the volume of the rock on the structure can be used.

The bottom elevation of the armor layer should be extended downslope to an elevation below minimum still-water level of at least one (significant) wave height, if the wave height is not limited by the water depth. Under depth limited conditions, the armor layer should be extended to the bottom as shown in Fig. 27 and supported by a toe.

4.2. *Rock armor layers*

Many methods for the prediction of rock size of armor units designed for wave attack have been proposed in the last 50 years. Those treated in more detail here are the Hudson formula as used in SPM (1984) and the formulas derived by Van der Meer (1988a).

4.2.1. *Hudson formula*

The original Hudson formula is written as

$$M_{50} = \frac{\rho_r H^3}{K_D \Delta^3 \cot \alpha} \,. \tag{45}$$

K_D is a stability coefficient taking into account all other variables. K_D values suggested for design correspond to a "no damage" condition where up to 5% of the armor units may be displaced. In the 1973 edition of the Shore Protection Manual, the values given for K_D for rough, angular stone in two layers on a breakwater trunk were

$K_D = 3.5$ for breaking waves,

$K_D = 4.0$ for nonbreaking waves.

The definition of breaking and nonbreaking waves is different from plunging and surging waves, which were described in Subsec. 2.1. A breaking wave in Eq. (45) means that the wave breaks due to the foreshore in front of the structure directly on the armor layer. It does not describe the type of breaking due to the slope of the structure itself.

No tests with random waves had been conducted and it was suggested that H_s in Eq. (54) was to be used. By 1984, the advice given was more cautious. The SPM now recommends $H = H_{1/10}$, being the average of the highest 10% of all waves. For the case considered above, the value of K_D for breaking waves was revised downward from 3.5 to 2.0 (for nonbreaking waves, it remained 4.0). The effect of these two changes is equivalent to an increase in the unit stone mass required by a factor of about 3.5!

The main advantages of the Hudson formula are its simplicity, and the wide range of armor units and configurations for which values of K_D have been derived. The Hudson formula also has many limitations. Briefly, they include

- potential scale effects due to the small scales at which most of the tests were conducted,
- the use of regular waves only,
- no account taken in the formula of wave period or storm duration,
- no description of the damage level,
- the use of nonovertopped and permeable core structures only.

The use of $K_D \cot\alpha$ does not always best describe the effect of the slope angle. It may therefore be convenient to define a single stability number without this $K_D \cot\alpha$. Further, it may often be more helpful to work in terms of a linear armor size, such as a typical or nominal diameter. The Hudson formula can be rearranged to

$$H_s/\Delta D_{n50} = (K_D \cot\alpha)^{1/3}. \tag{55}$$

Equation (55) shows that the Hudson formula can be written in terms of the structural parameter $H_s/\Delta D_{n50}$ which was discussed in Subsec. 2.3.1.

4.2.2. *Van der Meer formulas — deep water conditions*

Based on earlier work of Thompson and Shuttler (1975) an extensive series of model tests was conducted at Delft Hydraulics (Van der Meer (1987), (1988a) and (1988b)). These include structures with a wide range of core/underlayer permeabilities and a wider range of wave conditions. Two formulas were derived for plunging and surging waves, respectively, which are now known as the Van der Meer formulas:
for plunging waves,

$$\frac{H_s}{\Delta D_{n50}} = 6.2P^{0.18}\left(\frac{S}{\sqrt{N}}\right)^{0.2}\xi_m^{-0.5}\,, \tag{56}$$

and for surging waves,

$$\frac{H_s}{\Delta D_{n50}} = 1.0P^{-0.13}\left(\frac{S}{\sqrt{N}}\right)^{0.2}\sqrt{\cot\alpha}\,\xi_m^P\,. \tag{57}$$

The transition from plunging to surging waves can be calculated using a critical value of ξ_{mc}:

$$\xi_{mc} = [6.2P^{0.31}\sqrt{\tan\alpha}]^{\frac{1}{P+0.5}}\,. \tag{58}$$

For $\cot\alpha \geq 4.0$, the transition from plunging to surging does not exist and for these slope angles, only Eq. (56) should be used. All parameters used in Eqs. (56)–(58) are described in Sec. 2. The notional permeability factor P is shown in Fig. 6. The factor P should lie between 0.1 and 0.6.

Design values for the damage level S are shown in Table 4. The level "start" of damage, $S = 2-3$, is equal to the definition of "no damage" in the Hudson formula (Eq. (54)). The maximum number of waves N which should be used in Eqs. (56) and (57) is 7500. After this number of waves, the structure more or less has reached an equilibrium.

The wave steepness should lie between $0.005 < s_{om} < 0.06$ (almost the complete possible range). The mass density varied in the tests between 2000 kg/m^3 and 3100 kg/m^3, which is also the possible range of application.

The reliability of the formulas depends on the differences due to random behaviour of rock slopes, accuracy of measuring damage and curve fitting of the test results. The reliability of the Eqs. (56) and (57) can be expressed by giving the coefficients 6.2 and 1.0 in the equations a normal distribution with a certain standard deviation. The coefficient 6.2 can be described by a standard deviation of 0.4 (variation coefficient 6.5%) and the coefficient 1.0 by a standard deviation of 0.08 (8%). These values are significantly lower than that for the Hudson formula at 18% for K_D (with mean K_D of 4.5). With these standard deviations it is simple to include 90% or other confidence bands.

Equations (56)–(58) are more complex than the Hudson formula, Eqs. (54) or (55). They also include the effect of the wave period, the storm duration, the permeability of the structure, and a clearly-defined damage level. This may cause differences between the Hudson formula and Eqs. (56)–(58), which are illustrated hereafter.

The $H_s/\Delta D_{n50}$ in the Hudson formula is only related to the slope angle $\cot\alpha$. Therefore a plot of $H_s/\Delta D_{n50}$ or N_s versus $\cot\alpha$ shows one curve for

the Hudson formula. Equations (56)–(58) take into account the wave period (or steepness), the permeability of the structure, and the storm duration. The effect of these parameters are shown in Figs. 28 and 29. Figure 28 shows the curves for a permeable structure after a storm duration of 1000 waves (a little more than the number used by Hudson). Figure 29 gives the stability of an impermeable revetment after a wave attack of 5000 waves (equivalent to 5–10 hours in nature). Curves are shown for various wave steepnesses.

The conclusion is clear. The Hudson formula can only be used as a very rough estimate for a particular case. It should be borne in mind that a difference of a factor of two in the N_s-number means a difference in the stone mass of a factor of eight. These figures should be sufficiently convincing for the designer to apply Eqs. (56)–(58) instead of the simple Hudson formula.

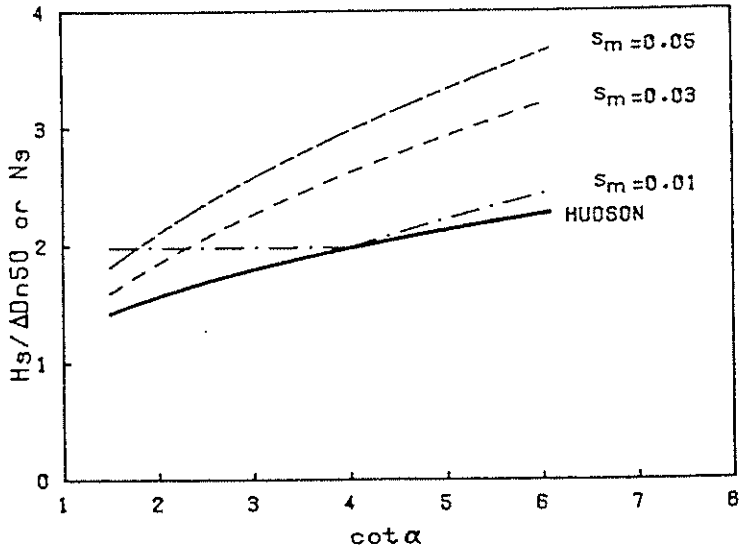

Fig. 28. Comparison between the Hudson formula and Eqs. (56)–(58) for a permeable core and after 1000 waves.

Nevertheless, it is more difficult to work with Eqs. (56)–(58). For a good design it is required to perform a sensitivity analysis for all parameters in the equations.

The deterministic procedure is to make design graphs where one parameter is evaluated. Three examples are shown in Figs. 30–32. Both give a wave height

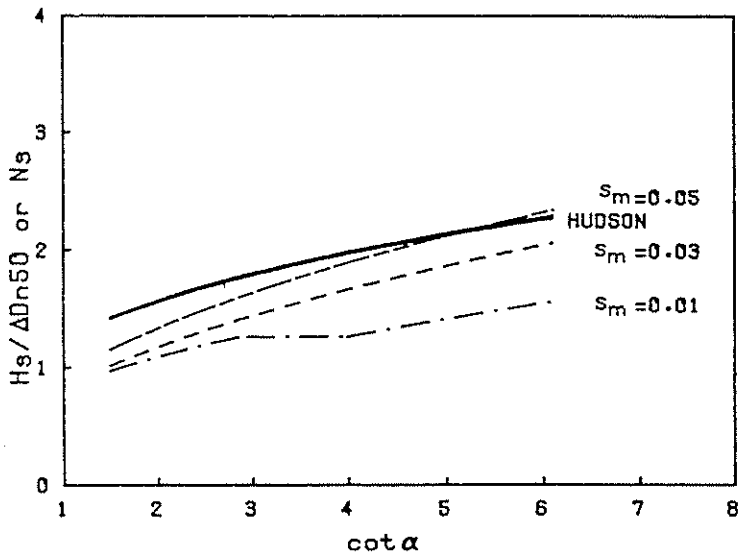

Fig. 29. Comparison between the Hudson formula and Eqs. (56)–(58) for an impermeable core and after 5000 waves.

versus surf similarity plot, which shows the influence of both wave height and wave steepness (the wave climate). The other shows a wave height versus damage plot which is comparable with the conventional way of presenting results of model tests on stability. The same kind of plots can be derived from Eqs. (56)–(58) for other parameters (see Van der Meer, 1988b).

The influence of the damage level S is shown in Fig. 30. Four damage levels are shown: $S = 2$ (start of damage), $S = 5$ and 8 (intermediate damage), and $S = 12$ (filter layer visible). The structure itself is described by $D_{n50} = 1.0\ m$ ($M_{50} = 2.6\,t$), $\Delta = 1.6, \cot\alpha = 3.0, P = 0.5$, and $N = 3000$.

The influence of the notional permeability factor P is shown in Fig. 32. Four values are shown: $P = 0.1$ (impermeable core), $P = 0.3$ (some permeable core), $P = 0.5$ (permeable core), and $P = 0.6$ (homogeneous structure). The structure itself is described by $D_{n50} = 1.0\ m$ ($M_{50} = 2.6\,t$), $\Delta = 1.6, \cot\alpha = 3.0$, $P = 0.5$, and $N = 3000$.

Damage curves are shown in Fig. 32. Two curves are given, one for a slope angle with $\cot\alpha = 2.0$ and a wave steepness of $s_{om} = 0.02$, and one for a

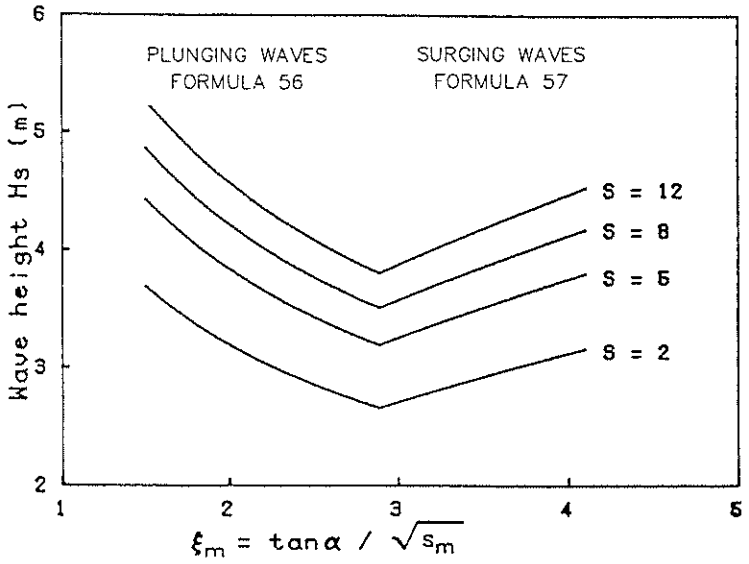

Fig. 30. Wave height versus surf similarity parameter; influence of damage level.

slope angle with $\cot\alpha = 3.0$ and a wave steepness of 0.05. If the extreme wave climate is known, graphs shown in Fig. 32 are very useful to determine the stability of the armor layer of the structure. Figure 32 shows also the 90% confidence levels which give a good idea about the possible variation in stability. This variation should be taken into account by the designer of a structure.

An estimation of the damage profile of a straight rock slope can be made by the use of Eqs. (56) and (57) and some additional relationships for the profile. The profile can be schematised to an erosion area around still-water level, an accretion area below still-water level, and for gentle slopes, a berm or crest above the erosion area. The transitions from erosion to accretion, etc., can be described by heights measured from still-water level (see Fig. 33). The heights are respectively h_r, h_d, h_m and h_b.

The relationships for the height parameters are based on the tests described by Van der Meer (1988a) and will not be given here. The assumption for the profile is a spline through the points given by the heights and with an erosion (and accretion) area according to the stability Eqs. (56) and (57). The method is only applicable for straight slopes.

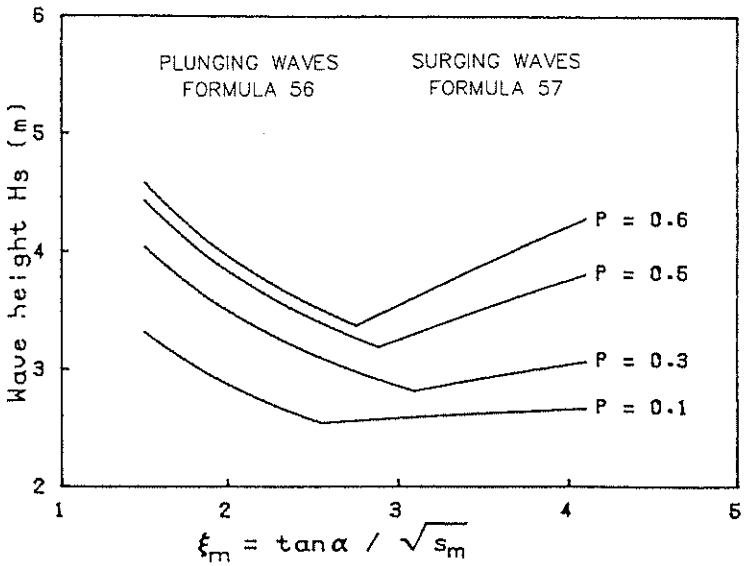

Fig. 31. Wave height versus surf similarity parameter; influence of permeability.

A deterministic design procedure is followed if the stability equations are used to produce design graphs as H_s versus ξ_m and H_s versus damage (see Figs. 30–32) and if a sensitivity analysis is performed. Another design procedure is the probabilistic approach. Equations (56) and (57) can be rewritten to so-called reliability functions and all the parameters can be assumed to be stochastic with an assumed distribution. Here, one example of the approach will be given. A more detailed description can be found in Van der Meer (1988b).

The structure parameters with the mean value, distribution type, and standard deviation are given in Table 8. These values were used in Level II first-order second-moment (FOSM) with the approximate full distribution approach (AFDA) method. With this method, the probability that a certain damage level would be exceeded in one year was calculated. These probabilities were used to estimate the probability that a certain damage level would be exceeded in a certain lifetime of the structure.

The parameter FH_s represents the uncertainty of the wave height at a certain return period. The wave height itself is described by a two-parameter Weibull distribution. The coefficients a and b take into account the reliability of the formulas, including the random behavior of rock slopes.

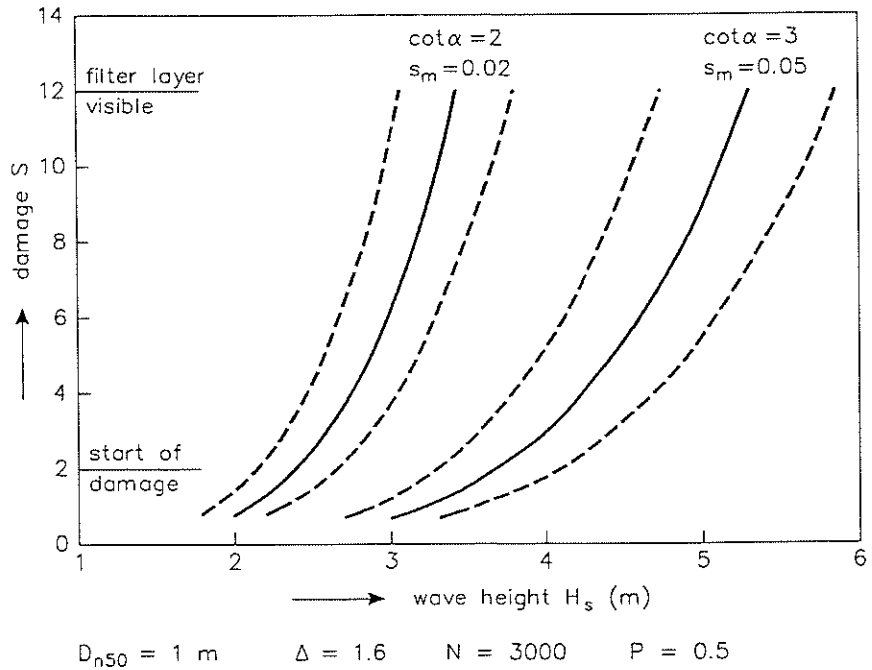

Fig. 32. Wave height versus damage.

Table 8. Parameters used in Level II probabilistic computations.

Parameter	Distribution	Average	Standard deviation
D_{n50}	Normal	1.0m	0.03m
Δ	Normal	1.6	0.05
$\cot\alpha$	Normal	3.0	0.15
P	Normal	0.5	0.05
N	Normal	3,000	1,500
H_s	Weibull	$B = 0.3$	$C = 2.5$
FH_s	Normal	0m	0.25m
s_{om}	Normal	0.04	0.01
a (Eq. 56)	Normal	6.2	0.4
b (Eq. 57)	Normal	1.0	0.08

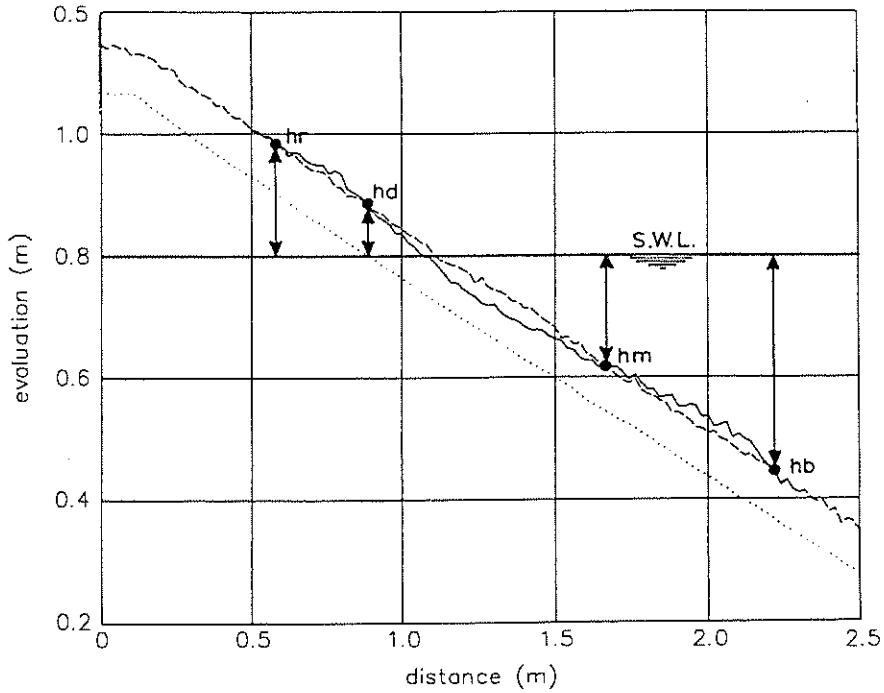

Fig. 33. Damage profile of a statically stable rock slope.

The final results are shown in Fig. 34 where the damage S is plotted versus the probability of exceedance in the lifetime of the structure. From this graph, it follows that the start of damage ($S = 2$) will certainly occur in a lifetime of 50 years. Tolerable damage ($S = 5$–8) in the same lifetime will occur with a probability of 0.2–0.5. The probability that the filter layer will become visible (failure) is less than 0.1. Probability curves as shown in Fig. 34 can be used to make a cost optimization for the structure during its lifetime, including maintenance and repair at certain damage levels.

Probabilistic Level II calculations as described above can easily be performed if the required computer programs are available. As this is not the case for many designers of breakwaters, it may be easier to use a Level I approach. This means that one applies design formulas with partial safety factors to account for the uncertainty of the relevant parameters. Most guidelines and building codes are based on a Level I approach. The determination of the

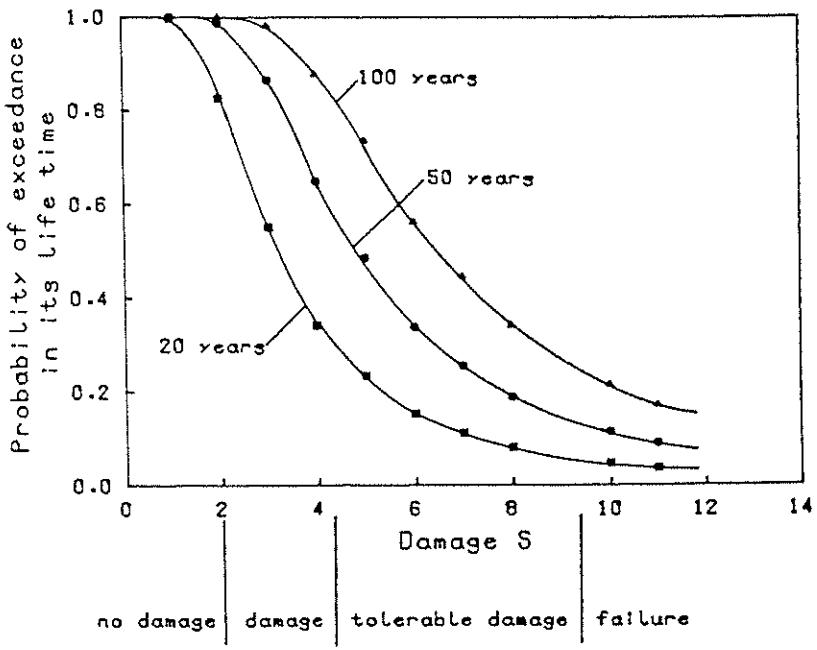

Fig. 34. Probability of exceedance of the damage level S in the lifetime of the structure.

partial safety factors is again based on Level II calculations, but this work has to be done by the composers of the guideline and not by the user.

The safety of rubble mound breakwaters has been described with a Level I approach (partial safety factors) in the recent PIANC report (1993). Two safety factors appeared to be enough to describe the uncertainty: one for the wave height and one for all other parameters together. Partial safety factors for most formulas in this paper are given in PIANC (1993).

4.2.3. *Shallow water conditions*

Up to now the significant wave height H_s has been used in the stability equations. In shallow water conditions, the distribution of the wave heights deviate from the Rayleigh distribution (truncation of the curve due to wave breaking). Further tests on a 1:30 sloping and depth limited foreshore by Van der Meer (1988a) showed that $H_{2\%}$ was a better value for design on depth limited foreshores than the significant wave height H_s, i.e., that the stability of the armor

layer in depth limited situations is better described by a higher characteristic value of the wave height distribution $H_{2\%}$ than by H_s.

Equations (56)–(58) can be rearranged with the known ratio of $H_{2\%}/H_s$ for a Rayleigh distribution. The equations become
for plunging waves,

$$\frac{H_{2\%}}{\Delta D_{n50}} = 8.7P^{0.18}\left(\frac{S}{\sqrt{N}}\right)^{0.2}\xi_m^{-0.5}\,, \tag{59}$$

and for surging waves,

$$\frac{H_{2\%}}{\Delta D_{n50}} = 1.4P^{-0.13}\left(\frac{S}{\sqrt{N}}\right)^{0.2}\sqrt{\tan\alpha}\,\xi_m^{P}\,. \tag{60}$$

Equations (59) and (60) take into account the effect of depth limited situations. A safe approach, however, is to use Eqs. (56) and (57) with H_s. In that case, the truncation of the wave height exceedance curve due to wave breaking is not taken into account which can be assumed as a safe approach. If the wave heights are Rayleigh distributed, Eqs. (59) and (60) give the same results as Eqs. (56) and (57), as this is caused by the known ratio of $H_{2\%}/H_s = 1.4$. For depth limited conditions, the ratio of $H_{2\%}/H_s$ will be smaller, and one should obtain information on the actual value of this ratio.

4.2.4. *Effects of armor shape and wide gradings*

The effects of armor shape on stability has been described by Latham *et al.* (1988). They tested five classes of rock with different shape classifications such as fresh, equant, semi-round, very round, and tabular. The damage to the test sections using each of the armor shapes tested was compared with damage calculated using Eqs. (56) and (57). As expected, very round rock suffered more damage than rock of other shapes. The performances of the fresh and equant rock were broadly similar. Surprisingly, the tabular rock exhibited higher stability than other armor shapes.

The coefficient 6.2 in Eq. (56) and 1.0 in Eq. (57) were used to describe the shape effects. These coefficients are summarised in Table 9.

Table 9. Revised coefficients for "nonstandard" armor shapes in Eqs. (56) and (57).

Rock shape class	Plunging waves Alternative for coefficient 6.2	Surging waves Alternative for coefficient 1.0
Fresh	6.32	0.81
Equant	6.24	1.09
Semi-round	5.96	0.99
Very round	5.88	0.81
Tabular	6.72	1.30

The stability of rock armor of (very) wide grading has been investigated by Allsop (1990). Model tests on a 1:2 slope with an impermeable core were conducted to identify whether the use of rock armor of grading wider than $D_{85}/D_{15} = 2.25$ will lead to armor performance substantially different from that predicted by Eqs. (56) and (57). The tests results confirmed the validity of these equations for rock of narrow grading ($D_{85}/D_{15} < 2.25$). Very wide gradings, such as $D_{85}/D_{15} = 4.0$, may in general suffer slightly more damage than predicted for narrower gradings. On any particular structure, there will be greater local variations in the sizes of the individual stones in the armor layer than for narrow gradings. This will increase spatial variations of the damage, giving a higher probability of severe local damage. Considerable difficulties will be encountered in measuring and checking such wide gradings. More information can be found in the above-mentioned references and in Allsop and Jones (1993).

4.3. *Armor layers with concrete units*

The Hudson formula (Eq. 55) was given in Subsec. 4.2 with K_D values for rock. The SPM (1984) gives a table with values for a large number of concrete armor units. The most important ones are $K_D = 6.5$ and 7.5 for cubes, $K_D = 7.0$ and 8.0 for tetrapods, and $K_D = 15.8$ and 31.8 for Dolosse. For other units, one is referred to SPM (1984).

Extended research by Van der Meer (1988c) on breakwaters with concrete armor units was based on the governing variables found for rock stability. The research was limited to only one cross-section (i.e., one slope angle and permeability) for each armor unit. Therefore, the slope angle, $\cot\alpha$, and consequently, the surf similarity parameter, ξ_m, is not present in the stability formulas developed on the results of the research. The same holds for the notional permeability factor, P. This factor was $P = 0.4$.

Breakwaters with armor layers of interlocking units are generally built with steep slopes in the order of 1:1.5. Therefore, this slope angle was chosen for tests on cubes and tetrapods. Accropode are generally built on a slope of 1:1.33, and this slope was used for tests on accropode. Cubes were chosen as these elements are bulky units which have good resistance against impact forces. Tetrapods are widely used all over the world and have a fair degree of interlocking. Accropode were chosen as these units can be regarded as the latest development, showing high interlocking, strong elements, and a one layer system. A uniform 1:30 foreshore was applied for all tests. Only for the highest wave heights which were generated, some waves broke due to depth limited conditions.

Damage to concrete units can be described by the damage number N_{od}, described in Subsec. 2.3.4. N_{od} is the actual number of displaced units related to a width (along the longitudinal axis of the breakwater) of one nominal diameter, D_n. N_{or} and N_{omov} are respectively the number of rocking units and the number of moving units (displaced + rocking).

As only one slope angle was investigated, the influence of the wave period should not be given in formulas including ξ_m, as this parameter includes both wave period (steepness) and slope angle. The influence of wave period, therefore, will be given by the wave steepness s_{om}. Final formulas for stability of concrete units include the relative damage level N_{od}, the number of waves N, and the wave steepness, s_{om}. The formula for cubes is given by

$$\frac{H_s}{\Delta D_n} = \left(6.7\frac{N_{od}^{0.4}}{N^{0.3}} + 1.0\right) s_{om}^{-0.1}, \tag{61}$$

for tetrapods,

$$\frac{H_s}{\Delta D_n} = \left(3.75\frac{N_{od}^{0.5}}{N^{0.25}} + 0.85\right) s_{om}^{-0.2}\ . \tag{62}$$

For the no-damage criterion $N_{od} = 0$, Eqs. (61) and (62) are reduced to

$$\frac{H_s}{\Delta D_n} = s_{om}^{-0.1}\ , \tag{63}$$

$$\frac{H_s}{\Delta D_n} = 0.85 s_{om}^{-0.2}\ . \tag{64}$$

The storm duration and wave period showed no influence on the stability of accropode and the "no damage" and "failure" criterions were very close. The

stability, therefore, can be described by two simple formulas:
start of damage, $N_{od} = 0$,

$$\frac{H_s}{\Delta D_n} = 3.7 \,, \tag{65}$$

failure, $N_{od} > 0.5$,

$$\frac{H_s}{\Delta D_n} = 4.1 \,. \tag{66}$$

A comparison of Eqs. (65) and (66) shows that the start of damage and failure of accropode are very close, although at very high $H_s/\Delta D_n$-numbers. It means that up to a high wave height, accropode are completely stable, but after the initiation of damage at this high wave height, the structure will fail progressively. Therefore, it is recommended that a safety coefficient for design of about 1.5 on the $H_s/\Delta D_n$-value be used. This means that for the design of accropode, one should use the following formula, which is close to design values of cubes and tetrapods:

$$\frac{H_s}{\Delta D_n} = 2.5 \,. \tag{67}$$

The reliability of Eqs. (61)–(66) can be described with a similar procedure as for rock. The coefficients 3.7 and 4.1 in Eqs. (65) and (66) for accropode can be considered as stochastic variables with a standard deviation of 0.2. The procedure for Eqs. (61)–(64) is more complicated. Assume a relationship:

$$\frac{H_s}{\Delta D_n} = a f(N_{od}, N, s_{om}) \,. \tag{68}$$

The function $f(N_{od}, N, s_{om})$ is given in Eqs. (61) and (62). The coefficient, a, can be regarded as a stochastic variable with an average value of 1.0 and a standard deviation. From this analysis, it follows that this standard deviation is $\sigma = 0.10$ for both formulas on cubes and tetrapods.

Equations (56) and (57) and (61)–(67) describe the stability of rock, cubes, tetrapods, and accropode. A comparison of stability is made in Fig. 35 where for all units curves are shown for two damage levels: "start of damage" ($S = 2$ for rock and $N_{od} = 0$ for concrete units) and "failure" ($S = 8$ for rock, $N_{od} = 2$ for cubes, $N_{od} = 1.5$ for tetrapods and $N_{od} > 0.5$ for accropode). The curves are drawn for $N = 3000$ and are given as $H_s/\Delta D_n$ versus the wave steepness, s_{om}.

From Fig. 35, the following conclusions can be drawn:

- "Start of damage" for rock and cubes is almost the same. This is partly due to a more stringent definition of "no damage" for cubes ($N_{od} = 0$). The damage level $S = 2$ for rock means that a little displacement is allowed (according to Hudson's criterion of "no damage", however).
- The initial stability of tetrapods is higher than for rock and cubes and the initial stability of accropode is much higher.
- Failure of the slope is reached first for rock, then cubes, tetrapods, and accropode. Stability at the "failure" level (in terms of $H_s/\Delta D_n$-values) is closer for tetrapods and accropode than at the initial damage stage.

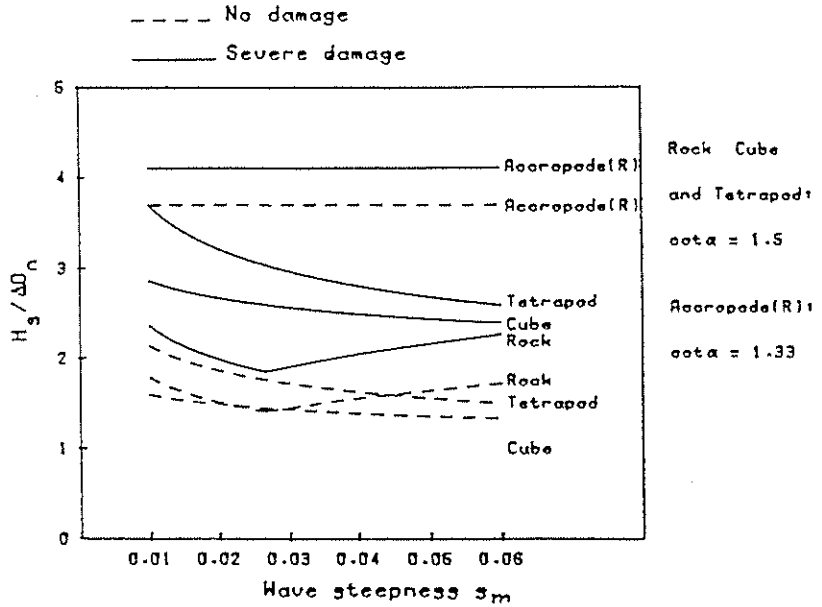

Fig. 35. Comparison of stability of rock, cubes, tetrapods, and accropode.

Another useful graph that can be directly derived from the stability formulas (61) and (62) is a wave height — damage graph. Figure 36 gives an example of cubes and gives the 90% confidence bands too, using the standard deviations described before.

Up to now damage to a concrete armor layer was defined as units displaced out of the layer (N_{od}). Large concrete units, however, can break due to limits

in structural strength. After the failures of the large breakwaters in Sines, San Ciprian, Arzew, and Tripoli, a lot of research all over the world was directed towards the strength of concrete armor units. The results of that research will not be described here.

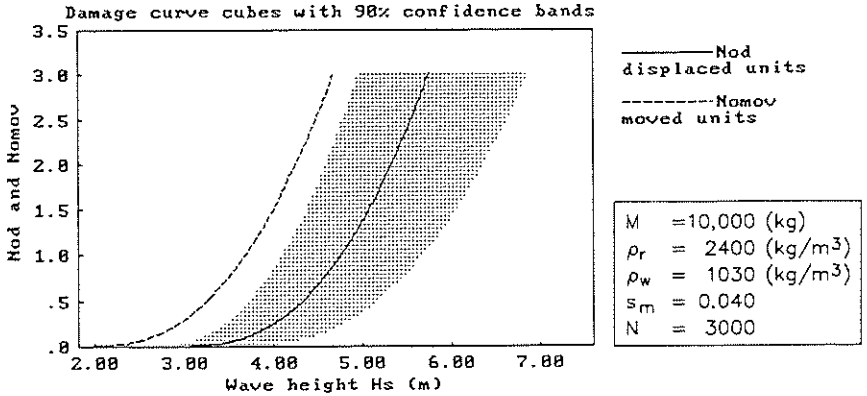

Fig. 36. Wave height — damage curve for cubes with 90% confidence levels.

In cases where the structural strength may play a role, however, it is interesting to know more than only the number of displaced units. The number of rocking units, N_{or}, or the total number of moving units, N_{omov}, may give an indication of the possible number of broken units. A (very) conservative approach is followed when one assumes that each moving unit results in a broken unit. The lower limits (only displaced units) for cubes and tetrapods are given by Eqs. (61) and (62). The upper limits (number of moving units) are derived by Van der Meer and Heydra (1990). The equations for the number of moving units are

for cubes,

$$\frac{H_s}{\Delta D_n} = \left(6.7\frac{N_{omov}^{0.4}}{N^{0.3}} + 1.0\right) s_{om}^{-0.1} - 0.5 \,, \tag{69}$$

for tetrapods,

$$\frac{H_s}{\Delta D_n} = \left(3.75\frac{N_{omov}^{0.5}}{N^{0.25}} + 0.85\right) s_{om}^{-0.2} - 0.5 \,, \tag{70}$$

The equations are very similar to Eqs. (61) and (62), except for the coefficient -0.5. In a wave height-damage graph, the result is a curve parallel to

the one for N_{od}, but which is shifted to the left. For armor layers with large concrete units, the actual number of broken units will probably lie between the curve of N_{od} (Eqs. (61) and (62)) and N_{omov} (Eqs. (69) and (70)).

Holtzhausen and Zwamborn (1992) investigated the stability of dolosse in a basic way, similar to the research on cubes, tetrapods, and accropode described above. Damage was defined as units displaced by more than one diameter and rocking or movements were not taken into account. The aspect of rocking (and breakage) should be considered for heavy dolosse, say, heavier than 10–15 t.

After some rewriting with respect to the damage number N_{od}, which is used in this paper, the stability formula for Dolosse becomes, according to Holtzhausen and Zwamborn (1992):

$$N_{od} = 6250 \left[\frac{H_s}{\Delta^{0.74} D_n}\right]^{5.26} s_{op}^3 w_r^{20 s_{op}^{0.45}} + E \,, \tag{71}$$

where

w_r = the waist ratio of the dolos,
E = error term.

The waist ratio w_r is a measure to account for possible breakage: a higher waist ratio gives a stronger dolos and should be used for relative severe wave attacks. The applicable range for the waist ratio is 0.33–0.40.

The error term E describes the reliability of the formula. It is assumed to be normally distributed with a mean of zero and a standard deviation of

$$\sigma(E) = 0.01936 \left[\frac{H_s}{\Delta^{0.74} D_n}\right]^{3.32} \,. \tag{72}$$

As Eq. (71) is a power curve, the no-damage criterion $N_{od} = 0$ cannot be substituted. According to Holtzhausen and Zwamborn (1992) no damage should be described as $N_{od} = 0.1$. The test duration was between 2000 and 3000 waves (one hour in the model). The influence of storm duration was not investigated, which means that Eq. (71) holds for storm durations in the same order as the tests.

Breakage of units has not been treated in this paper. Some relevant references on this topic are Burcharth *et al.* (1991), Burcharth and Liu (1992), Ligteringen *et al.* (1992), Scott *et al.* (1990), Van der Meer and Heydra (1991), and Van Mier and Lenos (1991).

4.4. *Underlayers, filters, toe protection, and head*

4.4.1. *Underlayers and filters*

Rubble mound structures in coastal and shoreline protection are normally constructed with an armor layer and one or more underlayers. Sometimes an underlayer is called a filter. The dimensions of the first underlayer depend on the structure type.

Revetments often have a two-diameter thick armor layer, a thin underlayer or filter, and then an impermeable structure (clay or sand), with or without a geotextile. The underlayer in this case works as a filter. Smaller particles beneath the filter should not be washed through the layer and the filter stones should not be washed through the armor. In this case the geotechnical filter rules are strongly recommended. Roughly, these rules give $D_{15}(\text{armor})/D_{85}(\text{filter}) < 4$ to 5.

Structures such as breakwaters have one or two underlayers followed by a core of rather fine material (quarry-run). The SPM (1984) recommends for the stone size of the underlayer under the armor a range of 1/10 to 1/15 of the armor mass. This criterion is more strict than the geotechnical filter rules and gives $D_{n50}(\text{armor})/D_{n50}(\text{underlayer}) = 2.2 - 2.3$.

A relatively large underlayer has two advantages. First, the surface of the underlayer is less smooth with bigger stones and gives more interlocking with the armor. This is especially so if the armor layer is constructed of concrete armor units.

Second, a large underlayer results in a more permeable structure and therefore has a large influence on the stability (or required mass) of the armor layer. The influence of the permeability on stability has been described in Subsec. 4.2.

Therefore, it is recommended that we use sizes of 1/10 to $1/15 M_{50}$ of the armor for the mass of the underlayer.

4.4.2. *Toe protection*

In most cases, the armor layer on the seaside near the bottom is protected by a toe (see Fig. 37). If the rock in the toe has the same dimensions as the armor, the toe will be stable. In most cases, however, one wants to reduce the rock size in the toe. Following the work of Brebner and Donnelly (1962), given in the SPM (1984), who tested toes to vertical-faced composite breakwaters under monochromatic waves, a relationship may be assumed between the ratio h_t/h and the stability number $H/\Delta D_{n50}$ (or N_s), where h_t is the depth of the toe below the water level and h is the water depth (also see Fig. 5). A small ratio of $h_t/h = 0.3$–0.5 means that the toe is relatively high above the bottom. In that case, the toe structure is more a berm structure. A value of $h_t/h = 0.8$ means that the toe is near the bottom.

Sometimes a relationship between $H_s/\Delta D_{n50}$ and h_t/H_s is assumed where a lower value of h_t/H_s should give more damage. Gravesen and Sørensen (1977) describe that a high wave steepness (short wave period) gives more damage to the toe than a low wave steepness. The above-mentioned assumption was based on only a few points. In the CIAD report (1985), this conclusion could not be verified. No relationship was found between $H_s/\Delta D_{n50}$ and h_t/H_s, probably because H_s is present in both parameters.

The CUR/CIRIA Manual (1991) gives a design graph on toe structure stability, based on a collection of site specific tests at Delft Hydraulics and the Danish Hydraulic Institute (see Fig. 37). Three damage classifications were defined: "0–3%" means no movement of stones (or only a few) in the toe; "3–10%" means that the toe flattened out a little, but the function of the toe (supporting the armor layer) is intact and the damage is acceptable. "Failure" means that the toe has lost its function and this damage level is not acceptable.

In almost all cases the structure was attacked by waves in a more or less depth limited situation, which means that H_s/h was fairly close to 0.5. This is also the reason why it is acceptable that the location of the toe, h_t, is related to the water depth, h. It would not be acceptable for breakwaters in very large water depths (more than 20–25 m). Figure 37 is, therefore, applicable for depth limited situations only.

Figure 37 shows that if the toe is high above the bottom (small h_t/h ratio), the stability is much smaller than for the situation where the toe is close to the bottom. The results of DHI (internal paper) are also shown in the graph and correspond well with the 3–10% values of Delft Hydraulics.

A suggested line for design purposes is given in the graph. In general, it means that the depth of the toe below the water level is an important parameter. If the toe is close to the bottom, the diameter of the stones can be more than twice as small as when the toe is half way down the bottom and the water level. A design formula for low and acceptable damage (3–10%) and for more or less depth limited situations is

$$\frac{H_s}{\Delta D_{n50}} = 8.7 \left(\frac{h_t}{h}\right)^{1.4} . \tag{73}$$

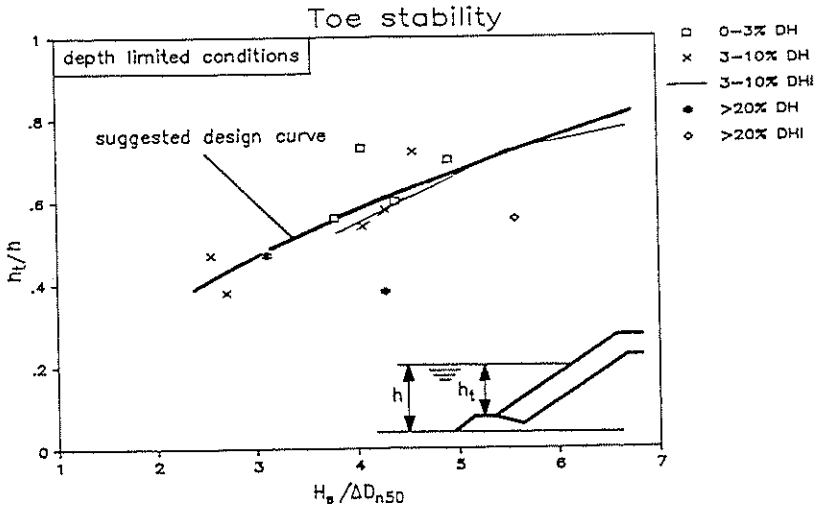

Fig. 37. Toe stability as a function of h_t/h.

Three points are shown in Fig. 37 which indicate failure of the toe. The above given design values are safe for $h_t/h > 0.5$. For lower values of h_t/h, one should use the stability formulas for armor stones described in Subsec. 4.2.

Recent research on toe structure stability was performed by Gerding (1993). His tests were performed in order to establish the influence of wave height, wave steepness, and water depth on toe stability. One of the main conclusions was that the wave steepness had no influence. His analysis resulted in an improved formula with regard to Eq. (73) and included the damage level N_{od} described earlier:

$$\frac{H_s}{\Delta D_{n50}} = \frac{H_{2\%}/1.4}{\Delta D_{n50}} = \left(0.24\frac{h_t}{D_{n50}} + 1.6\right) N_{od}^{0.15} \,. \tag{74}$$

In Eq. (74), $N_{od} = 0.5$ means start of damage, $N_{od} = 2$ means some flattening out, and $N_{od} = 4$ means complete flattening out of the toe. This applies to a "standard" toe size of about 3–5 stones wide and 2–3 stones high. For wider toe structures, a higher damage level can be applied before flattening out occurs. Equation (74) has no restrictions on depth limitation as the water depth h is not used as a parameter. The influence of limited water depth

(highest waves break) can be taken into account by using $H_{2\%}$ instead of H_s. A safe approach is followed when H_s is used. Equation (74) can be used in the range:

$0.4 < h_t/h < 0.9$,
$3 < h_t/D_{n50} < 25$.

4.4.3. *Breakwater head*

Breakwater heads represent a special physical process. Jensen (1984) described it as follows:

> "When a wave is forced to break over a roundhead it leads to large velocities and wave forces. For a specific wave direction only a limited area of the head is highly exposed. It is an area around the still-water level where the wave orthogonal is tangent to the surface and on the lee side of this point. It is therefore general procedure in design of heads to increase the weight of the armor to obtain the same stability as for the trunk section. Alternatively, the slope of the roundhead can be made less steep, or a combination of both."

An example of the stability of a breakwater head in comparison with the trunk section and showing the location of the damage, as described in the previous paragraph, is shown in Fig. 38 and was taken from Jensen (1984). The stability coefficient ($H_s/\Delta D_n$ for tetrapods) is related to the stability of the trunk section. Damage is located about 120°–150° from the wave angle. This local damage is clearly found by research with long-crested waves.

Possibly, the actual damage in prototype may be less concentrated as waves in nature are short-crested and multidirectional. Research in multidirectional wave basins should be undertaken to clarify this aspect.

No specific rules are available for the breakwater head. The required increase in weight can be a factor between 1 and 4, depending on the type of armor unit. The factor for rock is closer to 1.

Another aspect of breakwater heads is mentioned by Jensen (1984). The damage curve for a head is often steeper than for a trunk section. A breakwater head may show progressive damage. This means that if both head and trunk were designed on the same (low) damage level, an (unexpected) increase in wave height can cause failure of the head or a part of it, where the trunk still shows acceptable damage. This aspect is less pronounced for heads which are armored by rock.

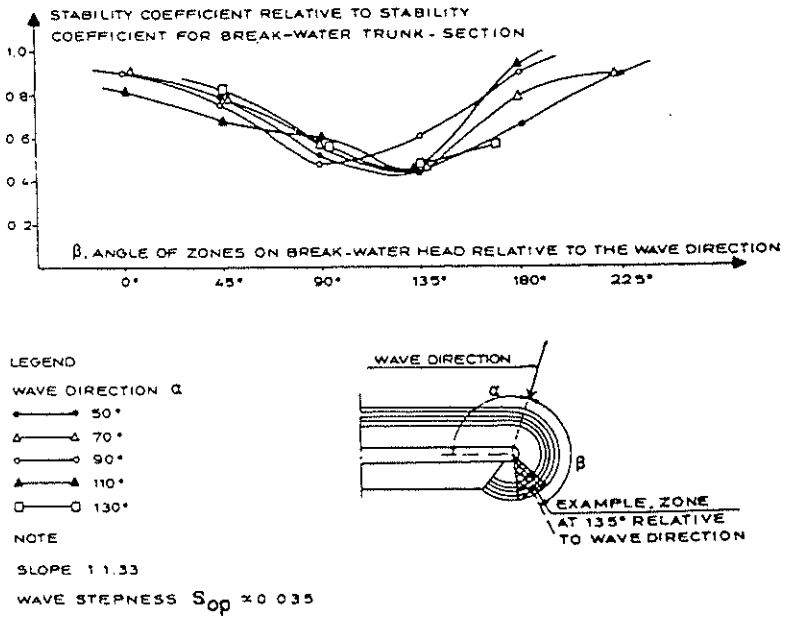

Fig. 38. Stability of a breakwater head armored with tetrapods. (Jensen, 1984)

4.5. *Crest and rear armor (low-crested structures)*

4.5.1 *Classification of low-crested structures*

As long as structures are high enough to prevent overtopping, the armor on the crest and rear can be (much) smaller than on the front face. The dimensions of the rock in that case will be determined by practical matters such as available rock, etc.

Most structures, however, are designed to have some or even severe overtopping under design conditions. Others are so low that under daily conditions, the structure is overtopped. Structures with the crest level around still-water level or below will always have overtopping and transmission.

It is obvious that when the crest level of a structure is low, wave energy can pass over the structure. This has two effects. First, the armor on the front side can be smaller than on a nonovertopped structure, due to the fact that less energy is left on the front side (lower run-down wave forces).

The second effect is that the crest and rear should be armored with rock which can withstand the attack by overtopping waves. For rock structures, the same armor on the front face, crest, and rear is often applied. The methods to establish the armor size for these structures will be given here. They may not hold for structures with an armor layer of concrete units. For those structures, physical model investigations may give an acceptable solution.

Low-crested rock structures can be divided into three categories: dynamically stable reef breakwaters, statically stable low-crested structures (with the crest above still-water level) and statically stable submerged structures.

A reef breakwater is a low-crested homogeneous pile of stones without a filter layer or core and is allowed to be reshaped by wave attack (Fig. 39). The initial crest height is just above the water level. Under severe wave conditions the crest height reshapes to a certain equilibrium crest height. This equilibrium crest height and the corresponding transmission are the main design parameters. The transmission was already described in Subsec. 3.3.

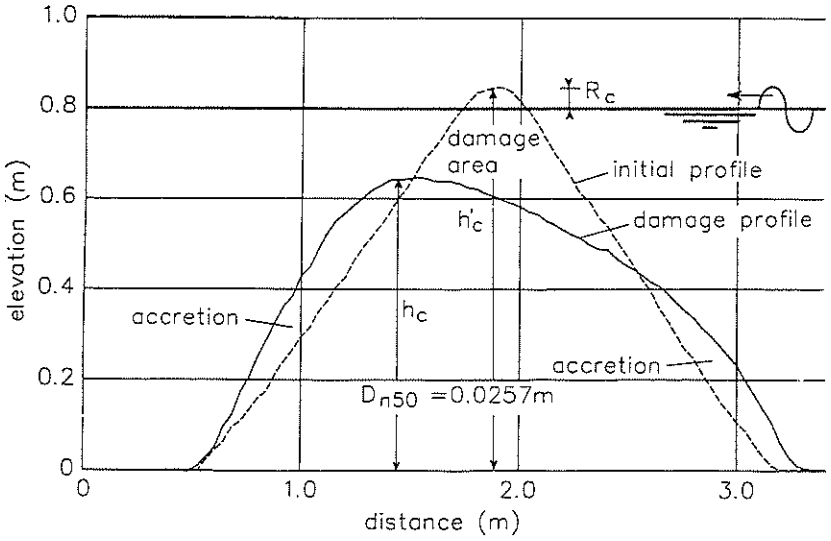

Fig. 39. Dynamically stable reef breakwater.

Statically stable low-crested breakwaters are close to non- or marginally overtopped structures, but are more stable due to the fact that a (large) part of the wave energy can pass over the breakwater (Fig. 40).

All waves overtop statically stable submerged breakwaters and the stability

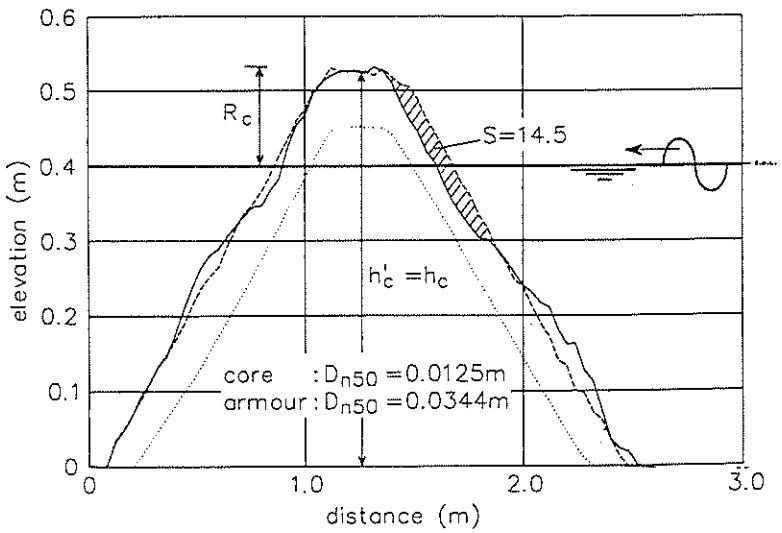

Fig. 40. Statically stable low-crested breakwater.

increases remarkably if the crest height decreases (Fig. 41). It is obvious that the wave transmission is substantial at these structures.

4.5.2. *Reef breakwaters*

The stability analyses conducted by Ahrens (1987, 1989) and Van der Meer (1990a) were concentrated on the change in crest height due to wave attack (see Fig. 39). Ahrens defined a number of dimensionless parameters which described the behavior of the structure. The main one is the relative crest height reduction factor h_c/h'_c. The crest height reduction factor h_c/h'_c is the ratio of the crest height at the completion of a test to the height at the beginning of the test. The natural limiting values of h_c/h'_c are 1.0 (no deformation) and 0.0 (structure not present anymore) respectively.

Ahrens found that for the reef breakwater, a longer wave period caused more displacement of material than a shorter period. Therefore, he introduced the spectral (or modified) stability number, N_s^*, defined by Eq. (9).

That a longer wave period results in more damage than a shorter period is not always true. Ahrens concluded that it is true for reef breakwaters where the crest height lowered substantially during the test. It is, however, not true

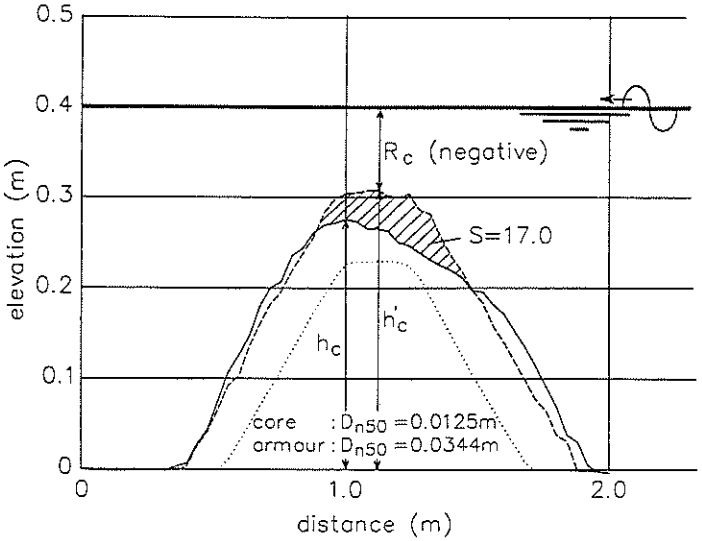

Fig. 41. Submerged breakwater.

for non- or marginally-overtopped breakwaters (Van der Meer, 1987 or 1988). The influence of the wave period in that case is much more complex than suggested by Eq. (9).

The (reduced) crest height, according to Van der Meer (1990a) or Van der Meer and Pilarczyk (1990) including all Ahrens' data, can be described by

$$h_c = \sqrt{\frac{A_t}{e^{aN_s^*}}} \tag{75}$$

with

$$a = -0.028 + 0.045C' + 0.34\frac{h'_c}{h} - 6.10^{-9}B_n^2 \tag{76}$$

and $h_c = h'_c$ if h_c in Eq. (75) $> h'_c$,
where

A_t = area of structure cross-section,
$C' = A_t/h'^2_c$ (structure response slope),
h = water depth at structure toe,
$B_n = A_t/D^2_{n50}$ (bulk number).

The lowering of the crest height of reef-type structures as shown in Fig. 39, can be calculated with Eqs. (75) and (76). It is possible to draw design curves from these equations which give the crest height as a function of N_s or even H_s. An example of h_c versus H_s is shown in Fig. 42. The reliability of Eq. (75) can be described by 90% confidence bands, given by $h_c \pm 5\%$ and is shown in Fig. 42.

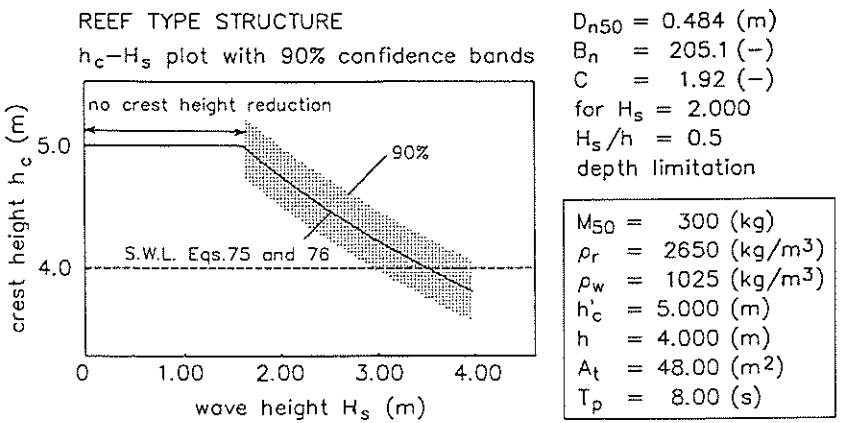

Fig. 42. Design graph of reef-type breakwater.

4.5.3. *Statically stable low-crested breakwaters*

The stability of a conventional low-crested breakwater above still-water level can be related to the stability of a non- or marginally-overtopped structure. For example, stability formulas such as (56) and (57) can be used. The required rock diameter for an overtopping breakwater can then be determined by the application of a reduction factor for the mass of the armor.

The derived equations are based on Van der Meer (1990a):
Reduction factor for

$$D_{n50} = \frac{1}{1.25 - 4.8R_p^*} \tag{77}$$

for $0 < R_p^* < 0.052$,
where

$$R_p^* = \frac{R_c}{H_s}\sqrt{\frac{s_{op}}{2\pi}} \,. \tag{78}$$

The R_p^* parameter is a combination of relative crest height, R_c/H_s, and wave steepness, s_{op}. Equation (77) describes the stability of a statically stable low-crested breakwater with the crest above still-water level simply by the application of a reduction factor on the required diameter of a nonovertopped structure (for example, according to Eqs. (56) and (57)). Equation (77) is shown in Fig. 43 for various wave steepnesses, and can be used as a design graph. The reduction factor to be applied for the nominal diameter can be read from this graph (or calculated by Eq. (77)).

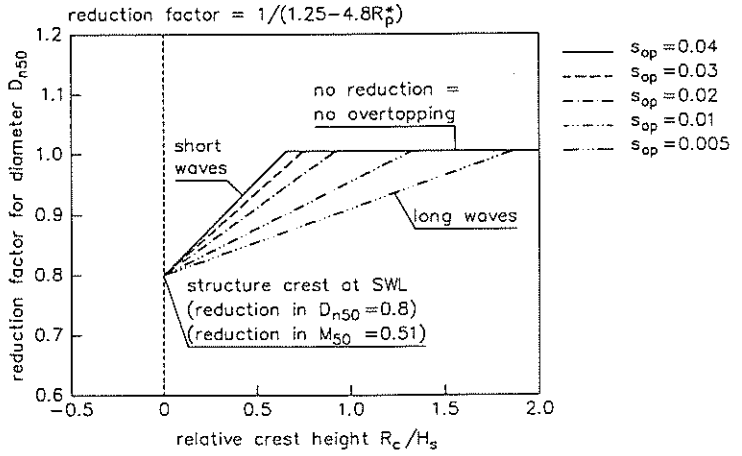

Fig. 43. Design graph for conventional low-crested structures above still-water level.

An average reduction factor of 0.8 in diameter is obtained for a structure with the crest height at the water level. The required mass in that case is a factor $0.8^3 = 0.51$ of that required for a nonovertopped structure.

It is not really required to describe the reliability of the reduction factor in Eq. (77). The reliability of D_{n50} is about the same as for a non- or marginally-overtopped structure, i.e., the reliability depends on the stability formula that is used to calculate the D_{n50} for a nonovertopped structure.

Vidal *et al.* (1992) studied a similar low-crested structure as described above (although including submerged structures), but they divided the armor layer of the structure into three sections: the front slope, the crest, and the back slope. These different sections of the structure have also different stability responses to a sea state condition. The behavior of the total slope protection

(as described by Eq. (77)), reflects the stability behavior of each section component. If one wants to optimize the armor weight to obtain a similar security condition in each part of the breakwater, the stability curves in each section should be determined.

Figure 44 gives a comparison of stability between the three sections as a function of the relative crest height and is taken from Vidal *et al.* (1992). The damage level that is described is $S = 2 - 2.5$ for each section (see Eq. (10)).

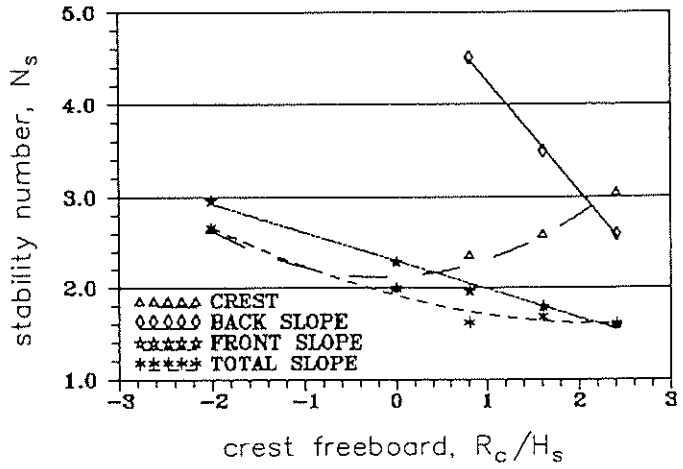

Fig. 44. Stability of front slope, crest, and back slope as a function of relative crest height. (Vidal *et al.*, 1992)

The front slope is least stable for relative crest heights of $R_c/D_{n50} > 0.5$. For $R_c/D_{n50} < 0.5$ the crest section is the least stable. The back slope is the most stable section for $R_c/D_{n50} < 2.0$. For larger values, the crest is more stable (although the stability should be similar for nonovertopped structures). If the freeboard is high (R_c/D_{n50} around 2.5) and the armor on the crest is the same as the back slope, the damage can start at the back slope and desegregate the crest.

The curve corresponding to the total slope reflects the basic principle of Eq. (77) and Fig. 43: the stability increases as the relative freeboard decreases. Moreover, the stability number for non- or marginally-overtopped structures in Fig. 44 amounts to $H_s/\Delta D_{n50} = 1.6$ and for structures with the crest at still-water level to $H_s/\Delta D_{n50} = 2.0$. This gives the same reduction factor of 0.8 for structures with the crest at the water line.

4.5.4. *Submerged breakwaters*

The slope angle has large influence on nonovertopped structures, but in the case of submerged structures the wave attack is concentrated on the crest and less on the seaward slope. Therefore, excluding the slope angle of submerged structures, being a governing parameter for stability may be legitimate.

The stability of submerged breakwaters appeared only to be a function of the relative crest height h'_c/h, the damage level S, and the spectral stability number N_s. The given formulas are based on a reanalysis of the tests of Givler and Sørensen (1986) by Van der Meer (1990a). The stability is described by

$$\frac{h'_c}{h} = (2.1 + 0.1S)e^{-0.14N_s^*} \quad . \tag{79}$$

For fixed crest height, water level, damage level, and wave height and period, the required ΔD_{n50} can be calculated from Eq. (79), finally yielding the required rock weight. Also, wave height versus damage curves can be derived from Eq. (79). The equation is shown as a design graph in Fig. 45 for four damage levels. The reliability of Eq. (79) can be described when the factor 2.1 is considered as a stochastic variable with a normal distribution. The data gives a standard deviation of 0.35. With this standard deviation, it is possible to calculate the 90% confidence bands, using $2.1 \pm 1.64 * 0.35$ in Eq. (79). Figure 45 gives the 90% confidence bands for $S = 2$. The scatter is quite large and this should be considered during the design of submerged structures.

4.6. *Berm breakwaters*

4.6.1. *Description of the seaward profile*

Statically stable structures can be described by the damage parameter S, (see Subsec. 2.3.4) and dynamically stable ones by a profile (see Fig. 8). Other typical profiles, but for different initial slopes, are shown in Fig. 46. The main part of the profiles is always the same. The initial slope (gentle or steep) determines whether material is transported upwards to a beach crest or downwards, creating erosion around the still-water level.

Based on extensive model tests (Van der Meer (1988a)), relationships were established between the characteristic profile parameters, as shown in Fig. 8,

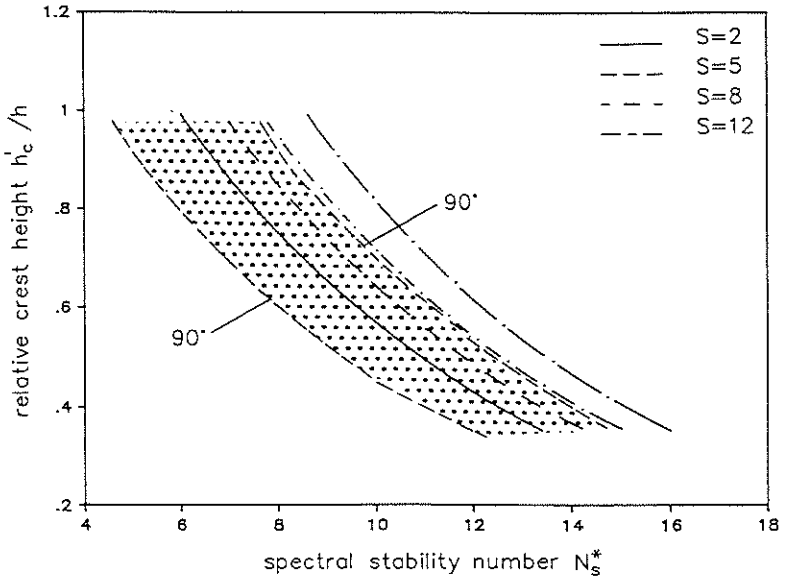

Fig. 45. Design curves for submerged breakwaters.

and the hydraulic and structural parameters. These relationships were used to make the computational model BREAKWAT, which simply gives the profile in a plot together with the initial profile. Boundary conditions for this model are

- $H_s/\Delta D_{n50}$ = 3-500 (berm breakwaters, rock and gravel beaches),
- arbitrary initial slope,
- crest above still-water level,
- computation of a (established or assumed) sequence of storms (or tides) by using the previously computed profile as the initial profile.

The input parameters for the model are the nominal diameter of the stone, D_{n50}, the grading of the stone, D_{85}/D_{15}, the buoyant mass density, Δ, the significant wave height, H_s, the mean wave period, T_m, the number of waves (storm duration), N, the water depth at the toe, h and the angle of wave incidence, β. The (first) initial profile is given by a number of (x, y) points with straight lines in between. A second computation can be made on the same initial profile or on the computed one.

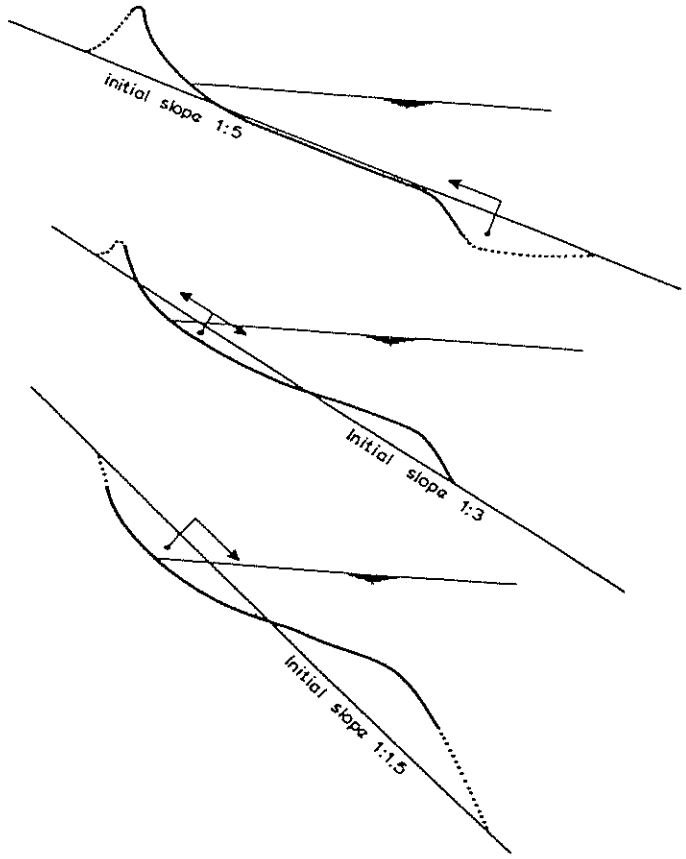

Fig. 46. Examples of profiles for different initial slopes.

The result of a computation on a berm breakwater is shown in Fig. 47, together with a listing of the input parameters. The model can be applied to

- design of rock slopes and gravel beaches,
- design of berm breakwaters,
- behavior of core and filter layers under construction during yearly storm conditions.

The computation model can be used in the same way as the deterministic design approach of statically stable slopes, described in Subsec. 4.2. There

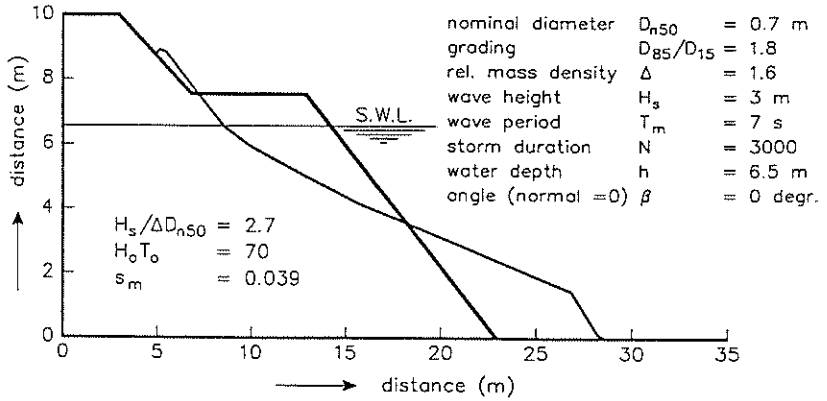

Fig. 47. Example of a computed profile for a berm breakwater.

the rather complicated stability Eqs. (56) and (57) were used to make design graphs such as damage curves, and these graphs were used for a sensitivity analysis. By making a large number of computations with the computational model, the same kind of sensitivity analysis can be performed for dynamically stable structures. Aspects which were considered for the design of a berm breakwater (Van der Meer and Koster (1988)) were, for example

- optimum dimensions of the structure (upper and lower slope, length of berm)
- influence of wave climate, stone class, water depth,
- stability after first storms.

An example to derive optimum dimensions for a berm breakwater will be described in the next section. The influence of the wave climate on a structure is shown in Fig. 48 and shows the difference in behavior of the structures for various wave climates. Stability after first (less severe) storms can possibly be described by the use of Eqs. (56) and (57).

Computations with the computational model can, of course, only be made if the model is available to the user. This is often not the case for the reader of a paper and therefore, a more simple (and less reliable) method should be given which is able to give the user a first impression (but not more than that!) of the profile that can be expected. This method is described below. Other estimates of profiles of gravel beaches are described by Powell (1990) and of berm breakwaters only by Kao and Hall (1990).

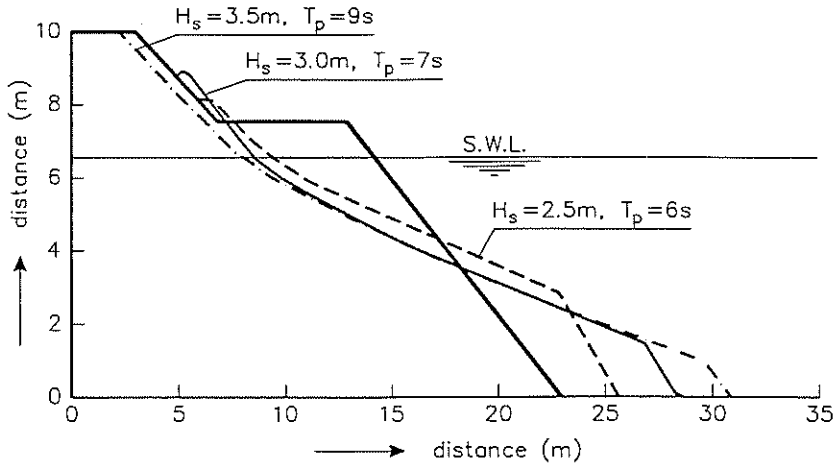

Fig. 48. Example of influence of wave climate on a berm breakwater profile.

Figure 49 gives the schematised profile simplified from the original profiles (see Fig. 8) in the computational model. The connecting point is the intersection of the profile with still-water level. From this point an upper slope is drawn under 1:1.8 and a lower slope under 1:5.5. The crest of the profile is situated on the upper slope and the transition to a steep slope on the lower part. These two points are given by the parameters l_c (length of crest) and l_s (length of step). Of course, a curved line goes through the three points.

The connection with the upper part of the profile and the initial profile is given by l_r (length of run-up). Below the gentle part under still-water level, a steep slope is present, and if the initial profile is gentle ($\cot\alpha > 4$) again there is a gentle slope which gives the "step" in the profile. The transition from a steep to a gentle slope is given by h_t (height of transition). If the initial slope is not a straight line, one should draw a more or less equivalent slope, taking into account the area from $+H_s$ to $-1.5H_s$, which gives $\tan\alpha$. The relationships between the profile parameters and the hydraulic and structural parameters are

$$l_c = 0.041 H_s T_m \sqrt{\frac{g}{D_{n50}}}\,, \tag{80}$$

$$l_s = l_r = 1.8\, l_c\,, \tag{81}$$

$$h_t = 0.6\, l_c\,. \tag{82}$$

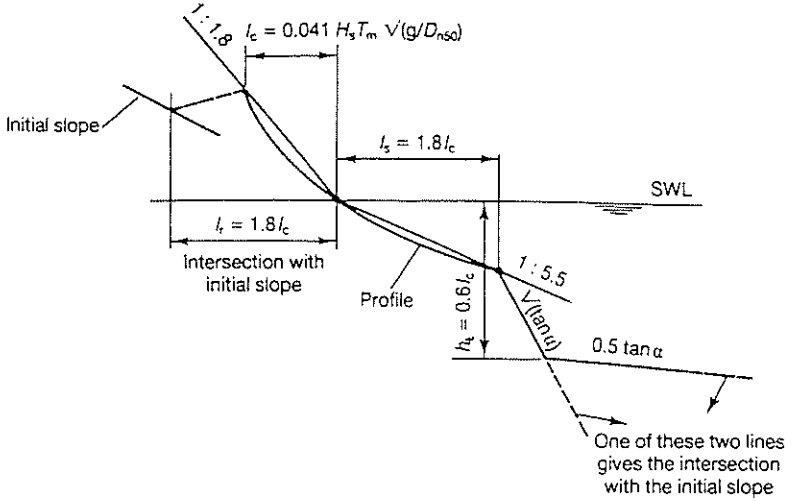

Fig. 49. Simple schematised profile for rock and gravel beaches.

$$\text{Steep slope below still-water level:} \sqrt{\tan\alpha}\ . \tag{83}$$

$$\text{Gentle slope below still-water level:} 0.5\tan\alpha\ . \tag{84}$$

Finally, the profile must be shifted along the still-water level until the mass balance is fulfilled. Figure 49 and Eqs. 80–84 give a rough indication of the profile that can be expected. For $H_s/\Delta D_{n50}$ values higher than about 10–15, the prediction is quite reliable. For lower values, the initial profile has a large influence on the profile and therefore, the given method is less reliable. This also applies to berm breakwaters and in that case the method should really be treated as a very rough indication.

4.6.2. *Optimum dimensions for a berm breakwater (example)*

A berm breakwater can be regarded as an unconventional design. Displacement of armor stones in the first stage of its lifetime is accepted. After this displacement (profile formation), the structure will be more or less statically stable. The initial cross-section of a berm breakwater can be described by a lower slope 1:m, a horizontal berm with a length b (just above still-water level in this case) and an upper slope 1:n. The lower slope is often steep and close to the natural angle of repose.

The critical design point in the example of Van der Meer and Koster (1988) was that erosion was not allowed on the upper slope above the berm. The minimum required berm length b was established for this criterion with the computational model. The berm length b was determined for various combinations of m and n. Figure 50 shows the final results. Each combination of m, n, and b from this graph gives more or less the same stability (no erosion on the upper slope). It is obvious from Fig. 50 that steep slopes require a longer berm and vice versa.

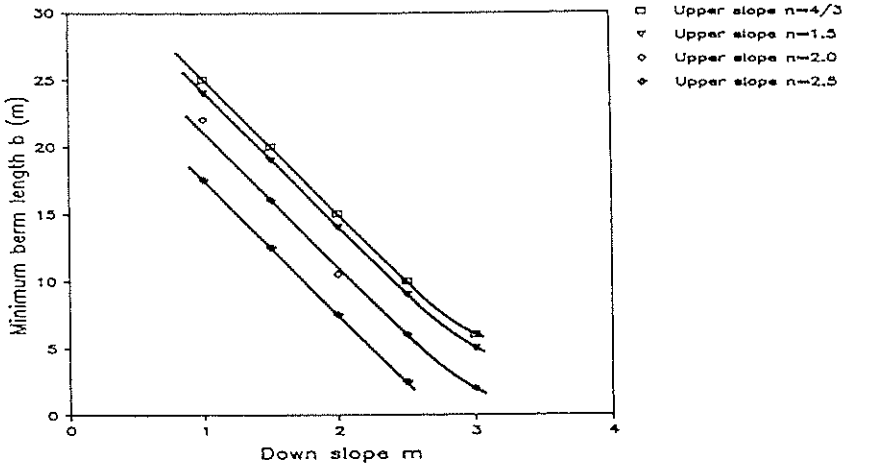

Fig. 50. Minimum berm length as a function of down slope and upper slope for a specific berm breakwater.

Figure 50 gives no information on the optimum values for the slopes. Therefore, another criterion is introduced. The amount of rock required for the construction was calculated for each combination of slopes and berm length. This amount of rock (or cross-sectional area), B, was plotted as a function of the upper and down slope and is given in Fig. 51. It shows that the down slope has minor influence on the required amount of rock (almost horizontal lines) and that a steep upper slope reduces this amount considerably.

It should be noted that actual values given in Figs. 50 and 51 were obtained for a specific structure with specific wave boundary conditions and that they are not generally applicable. But the trends and conclusions are.

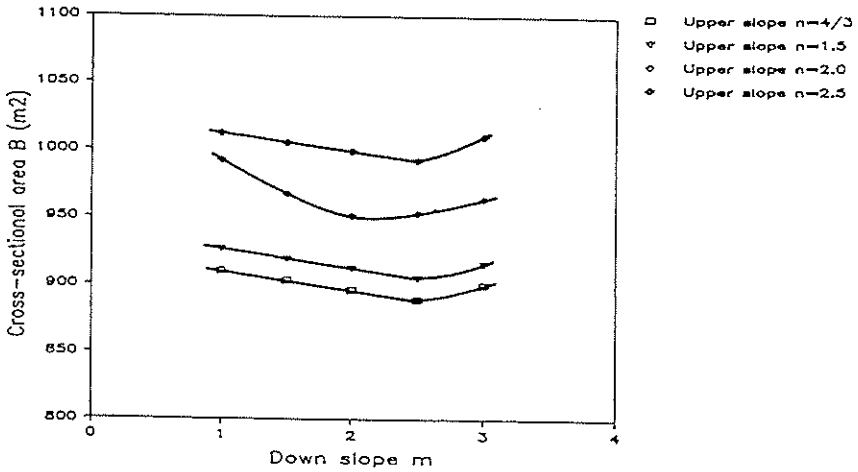

Fig. 51. Cross-sectional area as a function of down and upper slope for a specific berm breakwater.

The relationships for the computational model were based on tests in the range of $H_s/\Delta D_{n50} = 3$–500 (see Van der Meer (1988a)). The model was later verified specifically for berm breakwaters. This is described by Van der Meer (1990c). Tests from various institutes all over the world were used for this verification.

The overall conclusion was that the model never showed large unexpected differences with the test results and that in most cases the calculations and measurements were very close. Compaction of material caused by wave attack and damage to the rear of the structure caused by overtopping are not modeled in the program and this was and is a boundary condition for application of the program.

The combination of the statically stable formulas or model (Fig. 35) with the dynamically stable model showed to be a good tool for the prediction of the behavior of berm breakwaters under all wave conditions.

4.6.3. *Rear stability of berm breakwaters*

Van der Meer and Veldman (1992) performed extensive test series on two different berm breakwater designs. A first design rule was assessed on the relationship between damage to the rear of a berm breakwater and the crest height, wave height, wave steepness, and rock size.

The boundary condition is that the rock at the crest and rear of the berm breakwater has the same dimensions as at the seaward profile. This means that $H_s/\Delta D_{n50}$ is in the order of 3.0–3.5. A further restriction is that the profile at the seaward side has been developed into an S-shape.

The parameter, $R_c/{H_s}^* s_{op}^{1/3}$, showed to be a good combination of relative crest height and wave steepness to describe the stability of the rear of a berm breakwater. The following values of $R_c/{H_s}^* s_{op}^{1/3}$ can be given for various damage levels to the rear of a berm breakwater caused by overtopping waves and can be used for design purposes.

$$\begin{aligned} &\frac{R_c}{H_s} s_{op}^{1/3} = 0.25 : \text{ start of damage .} \\ &\frac{R_c}{H_s} s_{op}^{1/3} = 0.21 : \text{ moderate damage .} \\ &\frac{R_c}{H_s} s_{op}^{1/3} = 0.17 : \text{ severe damage .} \end{aligned} \tag{85}$$

A lower value of $R_c/{H_s}^* s_{op}^{1/3}$ means more overtopping and, therefore, more damage. Both a lower relative crest height R_c/H_s and a lower wave steepness give more overtopping and, therefore, more damage.

Andersen *et al.* (1992) performed basic tests on the stability of the rear of a berm breakwater. They included also undeveloped profiles and (very) long berms.

4.6.4. *Head of a berm breakwater*

Burcharth and Frigaard (1987) have studied longshore transport and stability of berm breakwaters in a short basic review. The recession of a breakwater head is shown as an example in Fig. 52, for fairly high wave attack ($H_s/\Delta D_{n50} = 5.4$). Burcharth and Frigaard (1987) state that, as a first rule of thumb for the stability of a breakwater head, $H_s/\Delta D_{n50}$ should be smaller than 3.

Tests on a berm breakwater head by Van der Meer and Veldman (1992) showed that increasing the height of the berm at this head and, therefore, creating a larger volume of rock, can be seen as a good measure for enlarging the stability of the round head of a berm breakwater, using the same rock as for the trunk.

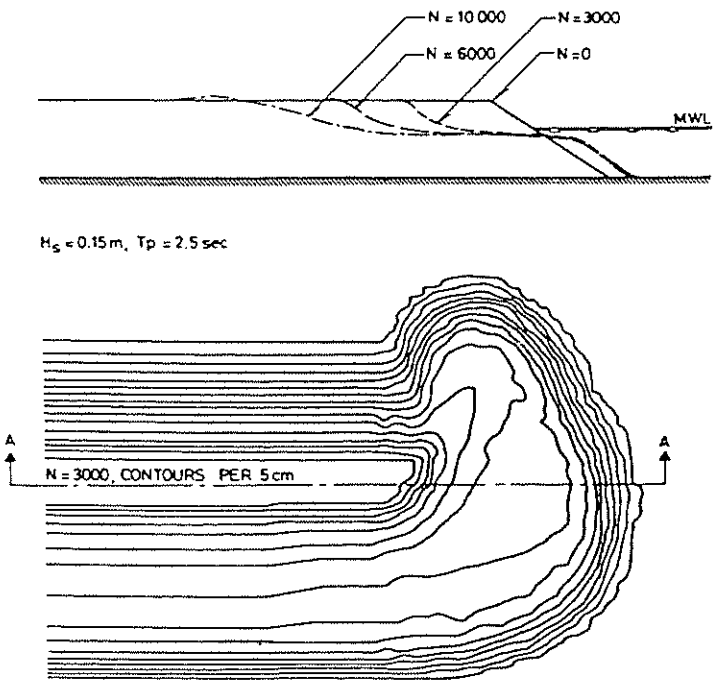

Fig. 52. Example of erosion of a berm breakwater head. (Burcharth and Frigaard, 1987)

4.6.5. *Longshore transport at berm breakwaters*

Statically stable structures as revetments and breakwaters are only allowed to show damage under very severe wave conditions. Even then, the damage can only be described by the displacement of a number of stones from the still-water level to (in most cases) a location downwards. Movement of stones in the direction of the longitudinal axis is not relevant for these types of structures.

The profiles of dynamically stable structures such as gravel/shingle beaches, rock beaches, and sand beaches change according to the wave climate. "Dynamically stable" means that the net cross-shore transport is zero and the profile has reached an equilibrium profile for a certain wave condition. It is possible that during each wave, material is moving up and down the slope (shingle beach).

Oblique wave attack generates wave forces parallel to the alignment of the structure. These forces can cause transport of material along the structure.

This phenomenon is called longshore transport and is well known for sand beaches. Also shingle beaches change due to longshore transport, although the research on this aspect has always been limited.

Rock beaches and berm breakwaters are or can also be dynamically stable under severe wave action. This means that oblique wave attack may induce longshore transport, which can also cause problems for these types of structures. Longshore transport does not occur for statically stable structures, but it will start for conditions where the diameter is small enough in comparison with the wave height. Then the conditions for the start of longshore transport are important.

The start of longshore transport is the most interesting consideration for the berm breakwater where profile development under severe wave attack is allowed, but longshore transport should be avoided. The berm breakwater can roughly be described by $2.5 < H_s/\Delta D_{n50} < 6$. Burcharth and Frigaard (1987) performed model tests to establish the incipient longshore motion for berm breakwaters and their range of tests corresponded to $3.5 < H_s/\Delta D_{n50} < 7.1$. Longshore transport is not allowed at berm breakwaters and, therefore, Burcharth and Frigaard gave the following (somewhat premature) recommendations for the design of berm breakwaters, which are in fact the criterions for incipient motion:

$$\begin{aligned} \text{for trunks exposed to steep waves, } & \frac{H_s}{\Delta D_{n50}} < 4.5 \ , \\ \text{for trunks exposed to oblique waves, } & \frac{H_s}{\Delta D_{n50}} < 3.5 \ , \\ \text{for roundheads, } & \frac{H_s}{\Delta D_{n50}} < 3 \ . \end{aligned} \tag{86}$$

Van der Meer and Veldman (1992) tested a berm breakwater under angles of wave attack of 25 and 50 degrees. Burcharth and Frigaard (1987, 1988) tested their structure under angles of 15 and 30 degrees. Longshore transport was measured by the movement of stones from a colored band. The transport was measured for developed profiles which meant that the longshore transport during the development of the profile of the seaward slope was not taken into account. The measured longshore transport, $S(x)$, was defined as the number of stones that was displaced per wave. Multiplication of $S(x)$ with the storm duration (the number of waves) in practical cases would lead to a transport rate of the total number of stones displaced per storm. Subsequently, the transport rate can be calculated in m^3/storm or m^3/s.

Figures 53 and 54 give all the test results on longshore transport, Both for the tests of Van der Meer and Veldman (1992) and the tests of Burcharth and Frigaard (1988). Both a higher wave height and a longer wave period result in larger transport. According to Eq. (8), a combined wave height-wave period parameter, $H_o T_{op}$, can be used:

$$H_o T_{op} = \frac{H_s}{\Delta D_{n50}} T_p \sqrt{\frac{g}{D_{n50}}} \,. \tag{87}$$

H_o is defined as the stability number, $H_s/\Delta D_{n50}$, and T_{op} as the dimensionless wave period related to the nominal diameter, $T_{op} = T_p\sqrt{g/D_{n50}}$. With the parameter, $H_o T_{op}$, it is assumed that wave height and wave period have the same influence on longshore transport. Figures 53 and 54 give the longshore transport $S(x)$ (in number of stones per wave) versus the $H_o T_{op}$.

Figure 53 gives all the data points. The maximum transport is about 3 stones/wave for $H_o T_{op} = 350$, which is in fact a very high rate for berm breakwaters. The $H_s/\Delta D_{n50}$-value in that case was 7.1, considerably higher than the design value for berm breakwaters. Figure 53 also shows that quite a number of tests had a much smaller transport rate than 0.1 – 0.2 stones/wave.

Therefore, Fig. 54 was drawn with a maximum transport rate of only 0.1 stones/wave. Now, only 4 data points remain of Burcharth and Frigaard (1988), the others are from the tests of Van der Meer and Veldman (1992).

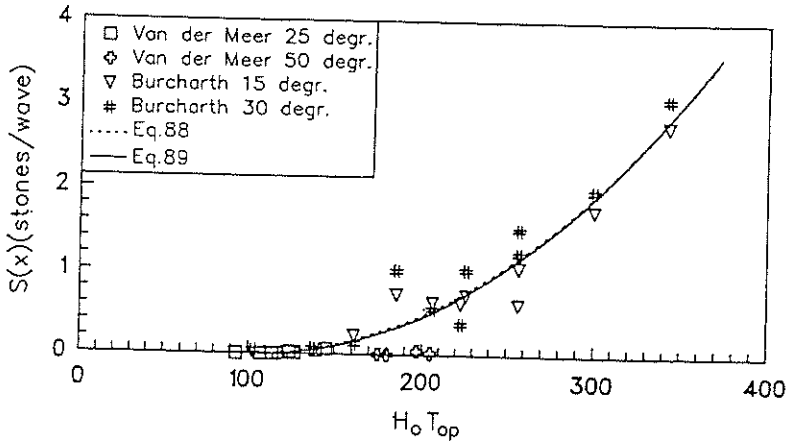

Fig. 53. Longshore transport for berm breakwaters.

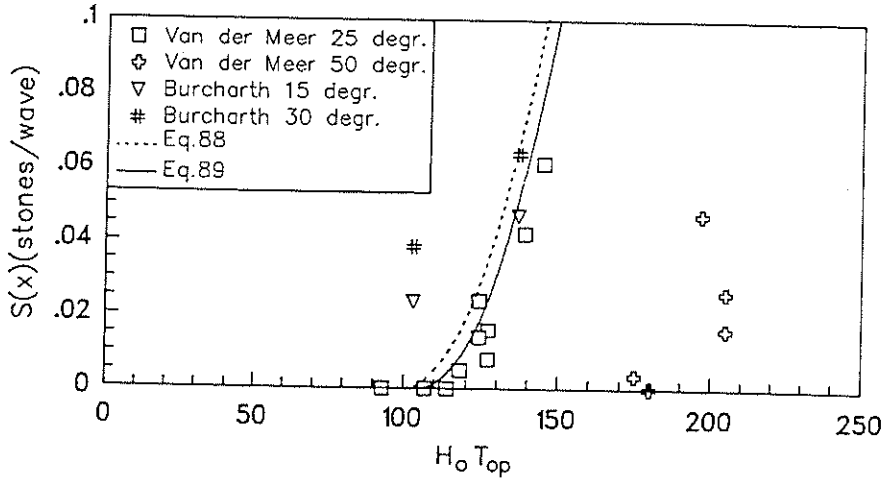

Fig. 54. Onset of longshore transport for berm breakwaters. This figure gives the exploded view of the part in Fig. 53 with $S(x) < 0.1$.

Figure 54 shows that the transport for large wave angles of 50 degrees is much smaller than for the other angles of 15–30 degrees. The two lowest points of Burcharth and Frigaard show transport for $H_o T_{op} = 100$, where the tests of Van der Meer and Veldman do not give longshore transport up to $H_o T_{op} = 117$.

Vrijling *et al.* (1991) use a probabilistic approach to calculate the longshore transport at a berm breakwater over its total lifetime. In that case, the start or onset of longshore transport is extremely important. They use the data of Van der Meer and Veldman (1992) and the data of Burcharth and Frigaard (1987), but not the extended series described in Burcharth and Frigaard (1988). Based on all data points, (except for some missing data points, these are similar to those in Fig. 53), they come to a formula for longshore transport:

$$\begin{aligned} &S(x) = 0 \text{ for } H_o T_{op} < 100 \,, \\ &S(x) = 0.000048(H_o T_{op} - 100)^2 \,. \end{aligned} \tag{88}$$

Equation (88) is shown in Figs. 53 and 54 with the dotted line. The equation fits nicely in Fig. 53, but does not fit the average trend for the low $H_o T_{op}$-region (see Fig. 54). The equation overestimates the start of longshore transport a little (except for 2 points of Burcharth and Frigaard). Therefore, Eq. (88) was

changed a little in order to describe the start of longshore transport better:

$$S(x) = 0 \text{ for } H_o T_{op} < 105 \,,$$
$$S(x) = 0.00005(H_o T_{op} - 105)^2 \,. \tag{89}$$

This equation holds for wave angles roughly between 15 and 35 degrees. For smaller or larger wave angles, the transport will be (substantially) less. Equation (89) is shown in Figs. 53 and 54 with the solid line and fits better in the low $H_o T_{op}$-region. The upper limit for Eq. (89) is chosen as $H_s/\Delta D_{n50} < 10$. With Eq. (89), the longshore transport for berm breakwaters has been established.

References

Ahrens, J. P. (1987). Characteristics of reef breakwaters. CERC, Vicksburg, Technical Report CERC-87-17.

Ahrens, J. P. (1989). Stability of reef breakwaters. *J. Wtrwy., Port, Coast. and Oc. Eng. ASCE.* **115**(2):221–234.

Allsop, N. W. H. and A. R. Channell (1989). Wave reflections in harbours: Reflection performance of rock armored slopes in random waves. Hydraulics Research, Wallingford, U.K., Report OD 102.

Allsop, N. W. H. (1990). Rock armoring for coastal and shoreline structures: Hydraulic model studies on the effects of armor grading. Hydraulics Research, Wallingford, U.K., Report EX 1989.

Allsop, N. W. H. and R. J. Jones (1993). Stability of rock armor and riprap on coastal structures. *Proc. Int. Riprap Workshop*, Fort Collins, Colorado, USA. 99–119.

Aminthi, P. and L. Franco (1988). Wave overtopping on rubble mound breakwaters. *Proc. 21st ICCE. ASCE.* Malaga, Spain.

Andersen O. H., J. Juhl, and P. Sloth (1992). Rear side stability of berm breakwater. *Proc. Final Overall Workshop of MAST G6S Coastal Structures*, Lisbon, Portugal.

Battjes, J. A. (1974). Computation of set-up, longshore currents, run-up, and overtopping due to wind-generated waves. *Comm. on Hydraulics*, Department of Civil Engineering, Delft Univeristy of Technology, Report 74–2.

Bradbury, A. P., N. W. H. Allsop, and R. V. Stephens (1988). Hydraulic performance of breakwater crown wall. Hydraulics Research, Wallingford, U.K., Report SR 146.

Brebner, A. and P. Donnelly (1962). Laboratory study of rubble foundations for vertical breakwater. Queen's University Kingston, Ontario, Canada, Engineer Report No. 23.

Burcharth, H. F. and P. Frigaard (1987). On the stability of berm breakwater roundheads and trunk erosion in oblique waves. *Seminar on Unconventional Rubble-Mound Breakwater. ASCE.* Ottawa, Canada.

Burcharth, H. F. and P. Frigaard (1988). On 3-dimensional stability of reshaping berm breakwaters. *Proc. 21st ICCE. ASCE.* Malaga, Spain. Ch. 169.

Burcharth, H. F., G. L. Howell, and Z. Liu (1991). On the determination of concrete armor unit stresses including specific results related to Dolosse. *J. Coast. Eng.* **15**:107–165.

Burcharth, H. F. and Z. Liu (1992). Design of Dolos armor units. *23rd ICCE. ASCE.* Venice, Italy. 1053–1066.

CIAD, Project group breakwaters (1985). Computer-aided evaluation of the reliability of a breakwater design, Zoetermeer, The Netherlands.

CUR/CIRIA Manual (1991). Manual on the use of rock in coastal and shoreline engineering. Gouda, The Netherlands, CUR Report 154. CIRIA special publication 83, London, U.K.

Daemen, I. F. R. (1991). Wave transmission at low-crested breakwaters. M.Sc. thesis. Delft University of Technology, Faculty of Civil Engineering, Delft, The Netherlands.

Daemrich, K. F. and W. Kahle (1985). Shutzwirkung von Unterwasserwellen brechern unter dem einfluss unregelmässiger Seegangswellen. Eigenverlag des Franzius-Instituts für Wasserbau und Küsteningenieurswesen, Heft 61 (in German).

De Gerloni, M., L. Franco, and G. Passoni (1991). The safety of breakwaters against wave overtopping. *Proc. ICE Conf. Breakwaters and Coastal Structures*, Thomas Telford, London, U.K.

De Waal, J. P. and J. W. Van der Meer (1992). Wave run-up and overtopping at coastal structures. *Proc. 23rd ICCE. ASCE.* Venice, Italy. 1758–1771.

Engering, F. P. H. and S. E. J. Spierenburg (1993). MBREAK: Computer model for the water motion on and inside a rubble and mound breakwater, Delft Geotechnics, MAST-G6S Report.

Franco, L. (1993). Overtopping of vertical face breakwaters: Results of model tests and admissible overtopping safes. *MAST 2-MCS-project Monolithic (vertical) Coastal Structures; Proc. of final workshop*, Madrid, Spain.

Führböter, A., U. Sparboom, and H. H. Witte (1989). Großer Wellenkanal Hannover: Versuchsergebnisse über den Wellenauflauf auf glatten und rauhen Deichböschungen mit de Neigung 1:6. Die Küßte. Archive for Research and Technology on the North Sea and Baltic Coast (in German).

Givler, L. D. and R. M. Sørensen (1986). An investigation of the stability of submerged homogeneous rubble-mound structures under wave attack. Lehigh University, H. R. IMBT Hydraulics, Report #IHL-110-86.

Gravesen, H. and T. Sørensen (1977). Stability of rubble mound breakwaters. *Proc. 24th Int. Navigation Congress*, Leningrad, Russia.

Holtzhausen, A. H. and J. A. Zwamborn (1992). New stability formula for dolosse. *23rd ICCE. ASCE.* Venice, Italy. 1231–1244.

Jensen, O. J. (1984). A monograph on rubble mound breakwaters. Danish Hydraulic Institute, Denmark.

Kao, J. S. and K. R. Hall (1990). Trends in stability of dynamically stable breakwaters. *Proc. 22nd ICCE. ASCE.* Delft, The Netherlands. Ch. 129.

Kobayashi, N. and A. Wurjanto (1989). Numerical model for design of impermeable coastal structures. University of Delaware, USA, Research Report No. CE-89-75.

Kobayashi, N. and A. Wurjanto (1990). Numerical model for waves on rough permeable slopes. *J. Coast. Res.*, Special issue 7:149–166.

Latham, J.-P., M. B. Mannion, A. B. Poole, A. P. Bradbury, and N. W. H. Allsop (1988). The influence of armorstone shape and rounding on the stability of breakwater armor layers. Queen Mary College, University of London, U.K.

Ligteringen, H., J. C. Van der Lem, and T. Silveira Ramos (1992). Ponta Delgada Breakwater Rehabilitation. Risk assessment with respect to breakage of armor units. *23rd ICCE. ASCE.* Venice, Italy. 1341–1353.

Owen, M. W. (1980). Design of seawalls allowing for wave overtopping. Hydraulics Research, Wallingford, U.K., Report No. EX 924.

PIANC (1993). Analysis of rubble mound breakwaters. Report of Working Group no. 12 of the Permanent Technical Committee II. Supplement to Bulletin No. 78/79. Brussels, Belgium.

Postma, G. M. (1989). Wave reflection from rock slopes under random wave attack. M.Sc. thesis. Faculty of Civil Engineering, Delft University of Technology, Delft, The Netherlands.

Powell, K. A. and N. W. H. Allsop (1985). Low-crest breakwaters, hydraulic performance and stability. Hydraulics Research, Wallingford, U.K., Report SR 57.

Powell, K. (1990). Predicting short term profile response for shingle beaches. Wallingford, U.K., Research Report SR 219.

Scott, R. D., D. J. Turcke, C. D. Anglin, and M. A. Turcke (1990). Static loads in Dolos armor units. *J. Coast. Res.*, Special issue 7:19–28.

Seelig, W. N. (1980). Two-dimensional tests of wave transmission and reflection characteristics of laboratory breakwaters. Vicksburg, USA, CERC Technical Report No. 80-1.

Seelig, W. N. (1983). Wave reflection from coastal structures. *Proc. Conf. Coastal Structures '83. ASCE.* Arlington, USA.

SPM (1984). Shore Protection Manual. Coastal Engineering Research Center. U.S. Army Corps of Engineers.

Steetzel, H. J. (1993). Cross-shore transport during storm surges. Ph.D. thesis. Delft University of Technology, Delft, The Netherlands.

TAW (1974). Technical Advisory Committee on Protection against Inundation. Wave run-up and overtopping. Government Publishing Office, The Hague, The Netherlands.

Thompson, D. M. and R. M. Shuttler (1975). Riprap design for wind wave attack. A laboratory study in random waves. HRS, Wallingford, U.K., Report EX 707.

Van der Meer, J. W. (1987). Stability of breakwater armor layers – Design formulas. Elsevier *J. Coast. Eng.* **11**:(3)219–239.

Van der Meer, J. W. (1988a). Rock slopes and gravel beaches under wave attack. Ph.D. thesis. Delft University of Technology, The Netherlands. Also, Delft Hydraulics Communication No. 396.

Van der Meer, J. W. (1988b). Deterministic and probabilistic design of breakwater armor layers. *Proc. ASCE, Wtrwy. Port, Coast. and Oc. Eng.* **114**(1):66–80.

Van der Meer, J. W. (1988c). Stability of cubes, tetrapods and accropode. *Proc. Breakwaters '88*, Eastbourne. Thomas Telford.

Van der Meer, J. W. and M. J. Koster (1988). Application of computational model on dynamic stability. *Proc. Breakwaters '88*, Eastbourne. Thomas Telford.

Van der Meer, J. W. and K. W. Pilarczyk (1990). Stability of low-crested and reef breakwaters. *Proc. 22th ICCE ASCE.* Delft, The Netherlands. 1375–1388.

Van der Meer, J. W. (1990a). Low-crested and reef breakwaters. Delft Hydraulics Report H 198/Q 638.

Van der Meer, J. W. (1990b). Data on wave transmission due to overtopping. Delft Hydraulics Report H 986.

Van der Meer, J. W. (1990c). Verification of BREAKWAT for berm breakwaters and low-crested structures. Delft Hydraulics Report H 986.

Van der Meer, J. W. and G. Heydra (1991). Rocking armor units: Number, location and impact velocity. Elsevier *J. Coast. Eng.* **15**(1 & 2):21–40.

Van der Meer, J. W. and K. d'Angremond (1991). Wave transmission at low-crested structures, in *Coastal Structures and Breakwaters Proc. ICE*, London, U.K. Thomas Telford.

Van der Meer, J. W. and J. J. Veldman (1992). Stability of the seaward slope of berm breakwaters. Elsevier *J. Coast. Eng.* **16**(2):205–234.

Van der Meer, J. W., H. A. H. Petit, P. Van den Bosch, G. Klopman, and R. D. Broekens (1992). Numerical simulation of wave motion on and in coastal structures. *Proc. 23rd ICCE. ASCE.* Venice, Italy. 1772–1784.

Van der Meer, J. W. and C. J. M. Stam (1992). Wave run-up on smooth and rock slopes of coastal structures. *J. Wtrwy., Port, Coast. and Oc. Eng. ASCE.* **118**(5):534–550.

Van der Meer, J. W. and I. F. R. Daemen (1994). Stability and wave transmission at low-crested rubble mound structures. *J. Wtrwy., Port, Coast. and Oc. Eng. ASCE.* **120**(1):1–19.

Van Gent, M. R. A. (1994). The modeling of wave action on and in coastal structures. Elsevier *J. Coast. Eng.* **22**(3 & 4):311–339.

Van Mier, J. G. M. and S. Lenos (1991). Experimental analysis of the load-time histories of concrete to concrete impact. Elsevier *J. Coast. Eng.* **15**(1 & 2):87–106.

Vellinga, P. (1986). Beach and dune erosion during storm surges. Ph.D thesis. Delft University of Technology, The Netherlands.

Vidal, C., M. A. Losada, R. Medina, E. P. D. Mansard, and G. Gomez-Pina (1992). A universal analysis for the stability of both low-crested and submerged breakwaters. *23rd ICCE. ASCE.* Venice, Italy. 1679–1692.

Vrijling, J. K., E. S. P. Smit, and P. F. De Swart (1991). Berm breakwater design; the longshore transport case: A probabilistic approach. *Proc. Coastal Structures and Breakwaters. ICE.* London, U.K. Thomas Telford.

Symbols

A_c	Armor crest freeboard, relative to still-water level
A_e	Erosion area on profile around still-water level
B	Structure width, in horizontal direction normal to face
C_r	Coefficient of wave reflection
C_t	Coefficient of total transmission, by overtopping or transmission through
D	Particle size, or typical dimension
D_n	Nominal block diameter $= (M/\rho_r)^{1/3}$
D_{n50}	Nominal diameter $(M_{50}/\rho_r)^{1/3}$
D	Sieve diameter
D_{50}	Sieve diameter, diameter of stone which exceeds the 50% value of sieve curve
D_{85}	85% value of sieve curve
D_{15}	15% value of sieve curve
D_{85}/D_{15}	Armor grading parameter
E_i	Incident wave energy
E_r	Reflected wave energy
E_t	Transmitted wave energy
F_c	Difference of level between crown wall and armor crest $= R_c - A_c$
G_c	Width of armor berm at crest
g	Gravitational acceleration
H	Wave height, from trough to crest
H_i	Incident wave height
H_{m0}	Significant wave height calculated from the spectrum $= 4\sqrt{m_0}$
H_r	Reflected wave height
H_t	Transmitted wave height
H_s	Significant wave height, average of highest one-third of wave height
$H_{2\%}$	Wave height exceeded by 2% of waves
$H_{1/10}$	Mean height of highest one-tenth of waves
H_oT_o	Dimensionless combined wave height-period parameter
h	Water depth
h_c, h'_c	Armor crest level relative to seabed, after and before exposure to waves
h_t	Depth of toe below still-water level
k_t	Layer thickness coefficient

L	Wave length, in the direction of propagation
L_o	Deep water or offshore wave length, $gT^2/2\pi$
M	Mass of an armor unit
M_{50}, M_i	Mass of unit given by 50%, i%, on mass distribution curve
m	Seabed slope
m_0	Zeroth moment of wave spectrum
m-nth	nth moment of spectrum
N	Number of waves in a storm, record or test
N_{od}, N_{od}, N_{omov}	Number of displaced, rocking, units per width D_n across armor face
N_s	Stability number $= H_s/\Delta D_{n50}$
N_s^*	Spectral stability number
P	Notional permeability factor, defined by van der Meer
P	Probability that x will not exceed a certain value; often known as cumulative probability density of x
p	Probability density of x
q	Overtopping discharge, per unit length of seawall
Q	Dimensionless overtopping discharge; various definitions
R	Strength descriptor in probabilistic calculations
R	Dimensionless freeboard parameters; various definitions
R_c	Crest freeboard, level of crest relative to still-water level
R_d	Run-down level, relative to still-water
$R_{d2\%}$	Run-down level, below which only 2% pass
R_u	Run-up level, relative to still-water level
$R_{u2\%}$	Run-level exceeded by only 2% of the incident waves
S	Loading descriptor in probabilistic design
S	Dimensionless damage, A_e/D_{n50}^2; may be calculated from mean profiles or separately for each profile line, then averaged
$S(x)$	Number of rocks displaced per wave in longshore direction
s	Wave steepness, H/L
s_{om}	Wave steepness for mean period, $2\pi H_s/gT_m^2$
s_{op}	Wave steepness for peak period, $2\pi H_s/gT_p^2$
s_p	Wave steepness with local wave length
T	Wave period
T_m	Mean wave period
T_p	Spectral peak period, inverse of peak frequency
t_a, t_u, t_f	Thickness of armor, underlayer or other layer

V	Variation coefficient $= \sigma/\mu$
Z	Reliability function in probabilistic design; $Z = R - S$
α	Structure front face angle
β	Angle of wave attack with respect to the structure
Δ	Relative buoyant density of material considered, e.g., for rock $= \rho_r/\rho_w - 1$
$\mu(x)$	Mean of x
ξ	Surf similarity parameter, or Iribarren number, $= \tan\alpha/\sqrt{s}$
ρ_r	Mass density (saturated surface dry density)
ρ_r, ρ_c, ρ_a	Mass density of rock, concrete, armor
ρ_w	Mass density of water
γ	Total reduction factor
γ_b	Reduction factor for a berm
γ_f	Reduction factor for rough slopes
γ_h	Reduction factor for depth limited waves
γ_β	Reduction factor for oblique wave attack
$\sigma(x)$	Standard deviation of x
ξ_m	Surf similarity parameter based on T_m
ξ_p	Surf similarity parameter based on T_p
ξ_{mc}	Critical surf similarly parameter